First 36 Cl cosmogenic moraine geochronology of the Dinaric mountain karst

Žebre, M.; Sarıkaya, M. A.; Stepišnik, U.; Yıldırım, C.; Çiner, A.

Published in:
Quaternary Science Reviews

DOI:
10.1016/j.quascirev.2019.02.002

Publication date:
2019

Citation for published version (APA):
Žebre, M., Sarıkaya, M. A., Stepišnik, U., Yıldırım, C., & Çiner, A. (2019). First ^{36}Cl cosmogenic moraine geochronology of the Dinaric mountain karst: Velež and Crvanj Mountains of Bosnia and Herzegovina. *Quaternary Science Reviews*, *208*, 54-75. https://doi.org/10.1016/j.quascirev.2019.02.002

First ^{36}Cl cosmogenic moraine geochronology of the Dinaric mountain karst: Velež and Crvanj Mountains of Bosnia and Herzegovina

[a,b]Žebre, M., [c]Sarıkaya, M.A., [d]Stepišnik, U., [c]Yıldırım, C., [c]Çiner, A.

[a]Geological Survey of Slovenia, Dimičeva ulica 14, 1000 Ljubljana, Slovenia

[b]Department of Geography & Earth Sciences, Aberystwyth University, United Kingdom (present address)

[c]Eurasia Institute of Earth Sciences, Istanbul Technical University, Maslak-Istanbul 34469, Turkey

[d]Department of Geography, Faculty of Arts, University of Ljubljana, Aškerčeva 2, 1000 Ljubljana, Slovenia

Corresponding author: Manja Žebre, manjazebre@gmail.com

Abstract

This article presents the first attempt to date moraines in the Dinaric mountain karst using cosmogenic ^{36}Cl surface exposure dating technique. Twenty samples were collected from moraine boulders from two sets of the lowest and largest lateral moraines on the Velež (1965 m asl) and Crvanj mountains (1920 m asl) in Bosnia and Herzegovina. The dated lateral-terminal moraine complexes, spanning elevations from ~980 to 1350 m asl, are up to 2.7 km long and rise more than 100 m above the valley floor. The moraine boulders yielded ^{36}Cl ages spanning from Oldest Dryas for Velež (14.9 ± 1.1 ka) to Younger Dryas for Crvanj (11.9 ± 0.9 ka), considering the average age of the two oldest samples from each lateral moraine as the most representative time of moraine emplacement. The dated moraines mark the largest extent of glaciers in both study areas, which have been reconstructed to ~ 28 km^2 for Velež and ~24 km^2 for Crvanj, having a mean equilibrium line altitude at 1388 m and 1541 m, respectively. Under modern precipitation values, which account for ~2000 mm, the temperature depression between 8 and 10 °C is required to sustain the palaeoglaciers with reconstructed equilibrium line altitudes. Glaciers of similar size with such low equilibrium line altitudes during the Lateglacial have not been reported until now for the Balkan Peninsula. It is very likely that the boulder ages reflect complex exhumation and denudation histories, which at this point do not allow obtaining more precise moraine chronologies for the study areas. Nevertheless, this article delivers new data on the extent and timing of Quaternary glaciations in the Mediterranean mountains, where records of glacier fluctuations seem to be asynchronous amongst different areas. It is clear that dating moraines with cosmogenic ^{36}Cl surface exposure dating in carbonate lithologies in areas of high precipitation like the Dinaric karst, remains challenging.

Keywords: Quaternary; Glaciation; Dinaric Karst; Cosmogenic Surface Exposure Dating; Equilibrium Line Altitude; Palaeoclimate

1. Introduction

The Dinaric Mountains is more than 650 km long mountain chain flanking the eastern Adriatic coast. It is characterised by a karst landscape with high-elevated plateaux, reaching the highest elevations in the central-southern belt (Čvrsnica – 2228 m asl (above sea level), Maglič - 2386 m asl, Durmitor – 2522 m asl, Prokletije - 2694 m asl). The highest parts of the Dinaric Mountains were glaciated during Pleistocene (Cvijić, 1899) and even today few small glacial remnants still exist in the Durmitor and Prokletije mountains (Gachev et al., 2016). Hence, this area is characterised by a combination of karst and glacial landscape (Telbisz et al., 2019; Žebre and Stepišnik, 2015).

Pioneer studies on past glaciations in the Dinaric Mountains were conducted at the end of the 19th century, focusing on the area of Montenegro and Bosnia and Herzegovina (e.g. Cvijić, 1899; Grund, 1902; Penck, 1900). Extensive monographs and scientific papers from that time hold detailed descriptions of glacial landforms and even reasonably precise geomorphological maps. In the 20th century the research on palaeoglaciations continued also in other Dinaric areas (e.g. Habič, 1968; Liedtke, 1962; Riđanović, 1966; Šifrer, 1959) with several interruptions owing to wars and political instabilities. These turbulent past events have left a great impact also on the recent state of knowledge on past glaciations in the Dinaric Mountains since majority of areas still remain undated (e.g. Krklec et al., 2015; Milivojević, 2007; Milivojević et al., 2008; Petrović, 2014) and without any detailed sedimentological and stratigraphic research. Nevertheless, it is not only the landmine contamination that prevents more detailed studies, but also dating glacial deposits in carbonate areas, with high precipitation gradients and hence important denudation rates (Levenson et al., 2017 and references therein), is still very challenging.

A number of techniques can be applied to date moraines and outwash deposits in carbonate environments, including U-series, luminescence, radiocarbon (^{14}C) and TCN (terrestrial cosmogenic nuclide) dating. U-series dating can be used to date secondary carbonates that are found cementing moraines and the practical range of this technique is ~350 ka (Hughes et al., 2013). The method relies

64 on several assumptions and criteria, where special care should be taken to ensure that samples are
65 from distinct crystal horizons and show no evidence of re-crystallisation and open-system behaviour
66 (Smart, 1991). Although the U-series method can provide only the age of the cement growth,
67 therefore lacking the precision needed to constrain the timing of moraine deposition, it was found to
68 be useful for bracketing moraines within certain glacial cycles in some of the Mediterranean
69 mountains (Hughes et al., 2011, 2010, 2006). Luminescence dating is often used to date outwash
70 sands and the upper age limit may extend up to 500 ka (Wallinga and Cunningham, 2015), but the
71 method is hardly applicable to carbonate environments owing to the lack of quartz and feldspars in
72 deposits (Krklec et al., 2015). Nevertheless, the method was successfully applied to some of the
73 carbonate-dominated landscapes in the Mediterranean, where smaller amounts of quartz were
74 present in outwash due to the limited exposures of non-carbonate bedrock in the glaciated
75 catchments (Bavec et al., 2004; Lewin et al., 1991). Although radiocarbon dating has a limited
76 chronological range (<50 ka) (Hughes et al., 2013), it has been shown to be a very robust method for
77 dating Last Glacial Maximum (LGM) moraines (e.g. Monegato et al., 2007) or other Late Pleistocene
78 glacial sequences even in limestone-dominated environments (e.g. Nieuwendam et al., 2016; Ruiz-
79 Fernández et al., 2016). However, in karstic terrains, this technique is commonly restricted either by
80 material availability in moraine matrix or by the hard-water error when applying the technique in
81 moraine-dammed lakes or bogs. Cosmogenic surface exposure dating with ^{36}Cl is an established
82 method for dating moraines (Dunai, 2010; Gosse and Phillips, 2001) and has been successfully
83 applied in carbonate environments elsewhere (e.g. Gromig et al., 2018; Pope et al., 2015; Sarıkaya et
84 al., 2014; Styllas et al., 2018). However, karst denudation rates limit the ^{36}Cl exposure dating
85 technique to be applied on carbonate lithologies that are exposed to extremely wet environmental
86 conditions, if they are older than ~40 ka (Hughes and Woodward, 2017).

87 Despite several methodological and physical obstacles such as landmines, it is important to obtain as
88 much data as possible on the glacial extent and chronology from the Dinaric Mountains and wider
89 Balkan area in order to better understand the temporally (a)synchronous maximum phase of

glaciation in the Mediterranean (Hughes and Woodward, 2017) and the past and present changes in atmospheric circulation influencing the Mediterranean region. The coastal Dinaric Mountains receive one of the highest precipitation amount in Europe today (Crkvice weather station - MAP (mean annual precipitation) ~ 5000 mm) and this seemed to be true also for the cold stage climates since according to the present state of knowledge one of the lowest equilibrium line altitudes (ELAs) in the Mediterranean were located in this area, showing a strong west-east gradient associated with westerlies (Hughes and Woodward, 2017). The Balkan area is also considered one of key areas for assessing the environmental and population history of Europe since it has been argued that this region served as a Lateglacial refugium for humans, animals and plants (Pilaar Birch and Vander Linden, 2018).

Although geomorphological evidence for palaeoglaciations in some of the Bosnia and Herzegovina Mountains has already been recognized in the 19th century (Cvijić, 1899), Bosnia and Herzegovina is considered as one of the main black spots in the Dinaric Mountains from the glacial chronological point of view, as there are no quantitative age data and detailed sedimentary analyses until today. In this paper we focus on the glacial chronology of the Velež and Crvanj mountains. Velež Mountain was recognized as glaciated for the first time by Grund (1902, 1910) in the early 20th century. In this very exact and advanced study for his time, considering the available topographic maps and other field instruments, Grund presented the geomorphological map of the northern side of Velež, including a detailed description of glacial features. He also estimated the snow line for the north-facing palaeoglaciers to be between 1350-1500 m asl. This area has been long time forgotten until 2015, when the glaciokarst phenomena were studied by Žebre and Stepišnik (2015). On the contrary, the Crvanj Mountain has never been studied before from a palaeoglaciological point of view. Therefore, the aims of our research are (a) to present the geomorphological and sedimentological evidence for glaciation on the Velež and Crvanj mountains, (b) to constrain the timing of the largest recognized glacier extent on Velež and Crvanj by applying the cosmogenic ^{36}Cl surface exposure dating technique for the first time in the Dinaric Mountains, (c) to reconstruct palaeoglacier dimensions and related

palaeo-ELAs, and (d) to critically evaluate a relevance of the obtained cosmogenic ages in the light of regional geomorphological and climate context.

2. Regional setting, geology and climate

The Velež and Crvanj mountains (43° 15'–43° 30' N and 17° 55'–18° 20' E) are located in the central Dinaric Mountains in southern Bosnia and Herzegovina between the Mostar basin to the west and Nevesinjsko polje to the south (Figure 1). The central mountain crest of Velež reaching elevations above 1700 m asl is approximately 12 km long and oriented in a NW-SE direction. The highest peak is Botin with 1965 m asl. On the other hand, the Crvanj Mountain has a plateau shape top with the highest elevations in its western part, where the peak of Zimomor reaches 1920 m asl.

The Velež Mountain is an overthrust of the Cretaceous shallow water carbonates over the Tertiary and Cretaceous sedimentary rocks (Hrvatović, 2005). The north-facing slopes, where majority of the research took place, are predominantly composed of Cretaceous limestone and dolostone. The Crvanj Mountain exhibits very similar geological features. Central part of the mountain is an overthrust of Triassic and Jurassic dolostones, with beds of limestone containing chert, overlying Jurassic and Cretaceous limestone (OGK, 1981, OGK, 1970). Owing to the prevalence of carbonate lithology, a well-developed karst aquifer functions within both areas. Subsurface drainage is oriented towards springs at the Nevesinjsko polje and other deep-entrenched valleys around the mountain, thus the vadose zone reaches depths of at least few hundred metres.

The study area is situated in a transition zone between the Mediterranean and continental climate, having characteristics of a warm temperate climate, fully humid, with cool summers (Cfc) according to the Köppen-Geiger climate classification (Kottek et al., 2006). Precipitation is well distributed throughout the year owing to the moisture coming from the Adriatic Sea (west) and the effect of orography. At Nevesinje (891 m asl), MAP over the period 1961-1990 was 1795 mm (Data courtesy

Federal Hydrometeorological Institute, Sarajevo), while MAP at higher elevations is likely to be higher; it was estimated to be up to 2000 mm (Vojnogeografski institut, 1969). The mean annual air temperature (MAAT) at Nevesinje is 8.6 °C with the warmest month being July (18 °C) and the coldest January (-0.9 °C).

Figure 1: (a) Study area and the topography of Mediterranean region after the mountain belts from Kapos et al. (2000) and (b) a close up of the southern Bosnia and Herzegovina. The study areas of the Velež and Crvanj mountains are located between Mostar basin to the west and Nevesinjsko polje to the south.

3. Methods

3.1 Geomorphological mapping

Field geomorphological mapping was carried out between 2012 and 2015. Topographic maps in a scale of 1:25.000 were used for mapping, while basic geological maps in a scale of 1:100.000 (OGK, 1981, OGK, 1970) were useful for giving a general support on the geological setting of the study area. With the exception of the northwestern area of Velež and northern part of Crvanj that are situated close or in the minefields (http://www.bhmac.org), the rest of the study area was examined in detail although the north-facing slopes of Velež below 1400 m asl are densely forested and therefore not easy to map. The interpretation of the spatially documented landforms on the field was supported by the sedimentological description of some outcrops, commonly exposed as road cuts or abandoned gravel pits. Standard field procedures (e.g. sedimentary structures, colour, clast size, distribution and roundness) and lithofacies codes following Evans and Benn (2004) were used for sediment description.

3.2 Cosmogenic nuclide dating

Cosmogenic ^{36}Cl surface exposure dating was used to infer the depositional ages of the moraines in the Velež and Crvanj mountains. The length of time that the boulder has been exposed on the moraine surfaces can be estimated by this method (Davis and Schaeffer, 1955; Dunai, 2010) via cosmogenically produced isotopes such as ^{36}Cl, ^{10}Be and ^{26}Al. Here, we used the ^{36}Cl because all lithologies, especially the carbonates, are suitable for the production mechanism of ^{36}Cl.

Dating with ^{36}Cl depends on the interactions between cosmic rays and nuclides in rocks. When rocks are exposed at or near surface, cosmic ray particles, which are secondary fast neutrons, thermal neutrons and negative slow muons start to bombard and interact with three main nuclides (^{40}Ca, ^{39}K and ^{35}Cl) to cause formation of cosmogenic ^{36}Cl. Therefore, measured ^{36}Cl concentrations in rocks can be used to quantify the time-length of boulder exposition (Gosse and Phillips, 2001; Owen et al., 2001).

3.2.1 Sample collection and chemical preparation

We collected 20 samples for cosmogenic ^{36}Cl dating from the top of the boulders on the crest of the moraines. The boulders were selected according to their positions on the crest, stability, size and preservation indicators; such imbedded large enough boulders on moraine crests were preferred. We concentrated on the largest moraines that were reasonably away from the minefields; hence safe enough to accomplish the fieldwork. We sampled on both right and left lateral moraines, targeting same number of samples from each lateral moraine. Only the largest glacial boulders with a stable position on the moraine crests have been taken into account. A hammer and chisel were used to take samples from upper few centimetres of the boulders and thicknesses of the samples were recorded (Table 1). Shielding of surrounding topography was measured by inclinometer from the horizon at each sample location (Gosse and Phillips, 2001). Sample locations were recorded by a hand-held GPS. Elevations data are also based on the GPS measurements except for BU samples, which are from topographic maps.

188 The rock samples were prepared at Istanbul Technical University (ITU) Kozmo-Lab
189 (http://www.kozmo-lab.itu.edu.tr/en) according to procedures described in Sarıkaya (2009). First,
190 samples were crushed and sieved to appropriate grain size (0.25-1 mm). Then they were leached
191 with deionized water and 10% HNO_3 to remove secondary carbonates, dust and organic particles.
192 Spiked (^{35}Cl enriched) samples were digested with excess amount of 2 M HNO3 in 500 ml HDPE
193 bottles (Sarıkaya et al., 2014; Schlagenhauf et al., 2010). ~10 ml of 0.1 M AgNO3 solution was added
194 before the digestion to precipitate AgCl. Later, isobar ^{36}S was removed from the solution by repeated
195 precipitation of $BaSO_4$ with addition of $Ba(NO_3)$ and re-acidifying with concentrated HNO_3. Final
196 precipitates of AgCl were sent to the ANSTO, Accelerated Mass Spectrometer (AMS) in Sydney,
197 Australia for isotope ratio measurements given in Supplementary Table S1.

198 Major element concentrations were determined with inductively coupled plasma emission
199 spectrometry (ICP-ES) and trace element concentrations with inductively coupled plasma mass
200 spectrometry (ICP-MS) at the Acme Lab (ActLabs Inc., Ontario Canada) to provide the total element
201 concentrations (Table 2). Total Cl was calculated by isotope dilution method (Desilets et al., 2006;
202 Ivy-Ochs et al., 2004) after AMS analysis (Table 2).

203 3.2.2 Determination of ^{36}Cl ages

204 The CRONUS Web Calculator version 2.0 (http://www.cronuscalculators.nmt.edu) (Marrero et al.,
205 2016a) was used to calculate sample ages. Cosmogenic ^{36}Cl production rates of Marrero et al.
206 (2016b) [56.3 ± 4.6 atoms ^{36}Cl (g Ca)-1 a-1 for Ca spallation, 153 ± 12 atoms ^{36}Cl (g K)-1 a-1 for K
207 spallation and 743 ± 179 fast neutrons (g air)-1 a-1] were used using the time-dependent Lifton-Sato-
208 Dunai scaling (also called “LSD” or “SF” scaling) (Lifton et al., 2014). We used 190 μ g-1 a-1 for slow
209 negative muon stopping rate at land surface at sea-level high-latitude (Heisinger et al., 2002). Lower
210 Ca spallation production rates suggested by Stone et al. (1996) or Schimmelpfennig et al. (2011) will
211 make our ages 7-10% older. Spallation and negative muon capture reactions are responsible for the
212 main production of ^{36}Cl (>95% for Mt. Velež samples and ~60% for Mt. Crvanj samples), with lesser

contributions from thermal neutron capture reactions by ^{35}Cl (5% for Mt. Velež samples and 40% for Mt. Crvanj samples). The chemical data (Table 2) and all other essential information including the ^{36}Cl concentrations and scaling factors to reproduce resultant ages is given in Table 3 and Supplementary Table S1.

All surface exposure ages include corrections for thickness and topographic shielding. We reported both zero-erosion and erosion corrected boulder ages (from 10 to 60 mm ka^{-1} of bedrock weathering assumed) and preferred to use the 40 mm ka^{-1} erosion corrected age, because the study area is located in one of the highest precipitation regions of Europe, and boulder surfaces show up to several cm deep solution grooves. Snow correction factor for spallation reactions of 0.9539 was applied to all samples based on snowpack of 25, 100, 100, 100, 50, 25 cm of snow on Nov, Dec, Jan, Feb, Mar and Apr on top of boulders. Snow thicknesses were estimated based on meteorological data from the Nevesinje weather station (Data courtesy Federal Hydrometeorological Institute, Sarajevo).

Table 1: Sample locations, attributes and local corrections to production rates.

Table 2: Geochemical and isotopic analytical data.

3.3 Glacier and climate reconstruction

3.3.1 Glacier geometry

A digitized geomorphological map of glacial features together with 20 m digital elevation model was used in the glacier geometry reconstruction. The glacier's extent was established using the field geomorphological evidence such as trimlines and lateral-frontal moraines. Then, the reconstruction was carried out by producing theoretical glacier surface profiles using the Profiler v.2 spreadsheet developed by Benn and Hulton (2010). We have largely followed the procedure presented in Žebre

238 and Stepišnik (2014), which is based on similar principles as the newly developed semi-automated
239 GlaRe GIS tool (Pellitero et al., 2016). Software ArcGIS 10.3.1 and a predefined *Topo to Raster*
240 interpolation method was used for calculating the ice surface with 50 m contour intervals.

241 3.3.2 Equilibrium Line Altitudes (ELA)

242 The equilibrium line altitude (ELA) of the reconstructed palaeoglaciers was determined by applying
243 the area altitude balance-ratio method (AABR) (Osmaston, 2005). The accumulation-area ratio (AAR)
244 method, which is the most widely used approach for the palaeo-ELA reconstruction, is becoming
245 increasingly replaced by the AABR method, which is also more reliable, provided that the correct
246 balance ratio is applied (Rea, 2009). The principle of the AABR method is that the total annual
247 accumulation above the ELA exactly balances the total annual ablation below the ELA under
248 equilibrium conditions (Benn and Gemmell, 1997). The advantage of this method is that explicitly
249 accounts for both glacier hypsometry and mass balance gradients (Benn and Gemmell, 1997). The
250 method gives the best results for the clean glaciers (Benn and Lehmkuhl, 2000) where most of them
251 will have the balance ratio between 1.5 and 3.5 (Osmaston, 2005). A representative balance ratio for
252 maritime mid-latitude glaciers is 1.9 ± 0.81 (Rea, 2009), which we applied for calculating the ELA of
253 palaeoglaciers on the Velež and Crvanj mountains. A GIS tool developed by Pellitero et al. (2015) was
254 used to facilitate the ELA calculations of individual valley, cirque and outlet glaciers. The latter were
255 separated by subdividing the ice field into sectors of individual glacier entities (Cowton et al., 2009;
256 Hughes et al., 2010). The local ELA of an individual mountain is represented as a mean ELA of the
257 entire group of glaciers. The ELA of each glacier was also estimated with the AAR method using a
258 ratio of 0.6, which is believed to be representative of valley and cirque glaciers (Benn and Evans,
259 1998; Nesje and Dahl, 2000; Porter, 1977). This allowed crosschecking the ELA results calculated with
260 the AABR method.

261 3.3.3 Temperature-melt simulations

For a better understanding of the relationship between glaciers and climate as well as an additional consideration of the age-dating results, we used a simple degree-day model (Brugger, 2006; Hughes, 2008), which calculates the amount of accumulation required to sustain glaciers. The inputs required for the model are mean annual temperature range and mean annual temperature. The latter is distributed over a sine curve to produce daily temperature means using the following equation (Brugger, 2006):

$$T_d = A_y sin(2\pi d/\lambda - \phi) + T_a$$

where T_d is the mean daily air temperature, A_y is the amplitude of the yearly temperature (½ of the annual temperature range), d the day of the year (1–365), λ is the period (365 days), ϕ is the phase angle (taken as 1.93 radians to reflect the fact that January is the coolest month) and T_a is the mean annual air temperature.

The annual accumulation required at the ELA to balance melting is equal to the sum of daily snowmelt, using a degree-day factor (Hughes et al., 2010). In our study we used the mean degree-day factor for snow of 4.1 mm day^{-1}°K^{-1}, which is representative of most glaciers and also in accordance with values reported in the literature (e.g. Braithwaite, 2008; Braithwaite et al., 2006). Snowmelt at the palaeo-ELAs on the Velež and Crvanj mountains was then reconstructed under different temperature regimes, using the climate data from Nevesinje (891 m asl) for the period 1961-1990. Mean annual temperature at this station was depressed by 4-15 °C in 1 °C intervals and then extrapolated to the mean palaeo-ELAs on Velež and Crvanj using the modern environmental lapse rate of 0.65 °C/100 m. The model was run using two different mean annual temperature ranges: the modern one (18.9 °C) and 150% of the modern range (28.35 °C). The latter reflects the possibility that palaeoclimate might have been more continental, since the sea level in the Adriatic basin was approximately 115 m lower at 20 ka, 100 m lower at 16 ka, and 60 m lower at 12 ka (Lambeck et al., 2011). Nevertheless, the above-described procedure allowed obtaining a range of

temperature-accumulation predictions and better understanding of the palaeoclimate needed to sustain glaciers in the study areas.

4. Results

4.1 Glacial geomorphology

4.1.1 Velež Mountain

The palaeoglacial landscape of the Velež Mountain (Figure 2a), with an emphasis on the glaciokarst features, was previously mapped by Žebre and Stepišnik (2015). The south-facing slopes exhibit minor glacier remodelling of the surface with only three cirques present below the highest peak Botin (1965 m asl). The cirque`s floors are situated between 1620 and 1790 m asl. A thin cover of glacial deposits is present on the cirque rims, while no glacial traces can be observed in lower elevations. On the contrary, the north-facing slopes are steep cliffs characterized by a series of cirques (Figures 3a and 3b) and extensive glacial deposition down to 950 m asl. Cirque floors on the northern side of Velež are situated much lower in elevation (between 1400 and 1500 m asl) from those on the south. Below cirques are polished limestone pavements and arêtes in between individual glacial valleys. Less than 5 km from the main mountain crest lateral-terminal moraine complexes occur at an elevation between 1300 and 1200 m.

We mapped 5 large lateral moraine pairs that are up to 2.7 km long and rise more than 100 m above the valley floor. Other two smaller moraine complexes are 1.1 km long and no more than 50 m high (Figure 2a). Moraines extend down to a minimum altitude of 940 m asl, where they are coupled with outwash fans. Breach-lobe moraines, formed by the glacier cutting through the main lateral moraines, are present on the external parts of some lateral-terminal moraine complexes, which are believed to be deposited by moraine-dammed glaciers, typical for the karst areas (Žebre and Stepišnik, 2015). Moraines occur also approximately 1 km up-valley of the outermost limits of glaciation and some 100 m higher. They are much smaller, indicating an evident shrinkage of glaciers

311 especially in ice thickness. In most valleys of the Velež Mountain, left- and right-lateral moraine
312 couples are common (Figure 2a). We did not recognize more than two clear sets of lateral moraines.
313 The third set is usually present only on the rim of some cirques.

314 Lateral moraines are composed of a diamicton (Dmm) characterized by a sandy-silty matrix and
315 subangular to subrounded cobble-to boulder sized clasts of Cretaceous limestone and dolostone.
316 Common boulders of ~1 m in diameter are scattered along the moraine crests, although those up to
317 3 m can be also found (i.e. sample BU16-06). Further down moraines two larger areas of outwash
318 deposition are present below 1000 m asl. The meltwaters from the glacial valleys west of the peak
319 Botin were directed towards the Donje Zijemlje karst depression (Figure 3c), while those from the
320 valleys east of the highest peak were running off towards Nevesinjsko polje. However, a bifurcation
321 of meltwaters below glaciers in the karst underground system is not excluded. Outwash fans are
322 slightly inclined, from 1.5° in the proximal zones to only 0.5° in the distal zones. They consist of
323 horizontally bedded, clast-supported gravels with rare sandy lenses (Gh). The clasts are subrounded
324 to rounded Cretaceous limestone and dolostone. Average size of the clasts is from 1 to 7 cm,
325 attaining a maximum of 17 cm.

326

327 Figure 2: (a) Geomorphological map of glacial landforms on the Velež Mountain. (b) Samples for ^{36}Cl
328 cosmogenic nuclide dating were collected from the Budijevača lateral-terminal moraine complex.
329 The samples ID`s along with the ages (ka) corrected for 40 mm ka^{-1} of erosion are presented in (b).

330

331 Figure 3: (a) Steep north-facing slopes of the Velež Mountain showing a series of cirques in the upper
332 parts and moraines entirely covered by forest below them. (b) The easternmost cirque on the Velež
333 Mountain, which hosted a small valley glacier during the maximum glacial phase. (c) The
334 westernmost outwash fan filling the floor of Donje Zijemlje karst depression.

335

4.1.2 Crvanj Mountain

The western slopes of the Crvanj Mountain (Figure 4a) were remodelled by limited extent of a cirque-type glaciation. A complex of three cirques (Figure 5a) with northwestern exposition are present below the highest peak Zimomor (1920 m asl). The cirque floors are situated at an elevation span of 1430-1480 m asl. Up to 10 m high moraine ridges are located inside and below the cirques between 1400 and 1500 m asl. Three km long, deeply entrenched gully starts below glacial deposits and terminates in the apex of the large outwash fan, covering the northern part of Nevesinjsko Polje.

Central part of the mountain is a wide-ranging plateau, having surface slightly sloping eastwards. Major part of the plateau area is made of dolostone that appears to be glacially moulded, showing rounded hills slightly elongated in the direction of glacier flow, and few dolines and polished pavements. Only limited patches of glacial till can be found on the plateau, whereas on the eastern and southern slopes of Crvanj glacial till appears in the form of large lateral moraines. The northern sector of the mountain, where glacial deposits are also to be expected, has not been examined on the field due to the presence of minefields. Since the area is completely overgrown by a forest, it was neither possible to confirm the presence of moraines by means of remote sensing data.

A pair of lateral moraines and minor recessional moraines on the south-facing slopes extend between 1180 and 1400 m asl. In between the main lateral moraines, a gully is carved in bedrock, and after approximately 3 km of length it terminates in the outwash fan on Nevesinjsko Polje. The largest moraines that were also sampled (Figure 4b), are present on the eastern slopes of Crvanj at an elevation range of ~1000-1350 m asl. Lateral moraines are no more than 1.5 km long and rise up to 150 m above the terminal moraine depression, where a lake is present (Figure 5b).

Till building these lateral moraines appears as a diamicton (Dmm) with sandy-silty matrix and angular to subrounded clasts (Figure 5c). The lithology is more diverse as in the case of the Velež moraines. Limestone and dolostone clasts show greater roundness compared to sandstone clasts (Figure 5d), which are often striated. Gravel- to boulder sized clasts prevail within examined outcrops, while scarce

boulders, not exceeding 1.5 m in height, can be observed on the crests of moraines. Outwash deposits in the Crvanj area have not been examined in detail due to a lack of outcrops.

Figure 4: (a) Geomorphological map of glacial landforms on the Crvanj Mountain. (b) Samples for ^{36}Cl cosmogenic nuclide dating were collected from the Jezero left and right lateral moraines. The samples ID`s along with the ages (ka) corrected for 40 mm ka^{-1} of erosion are presented in (b).

Figure 5: (a) Northern cirque below the highest peak of the Crvanj Mountain. (b) The sampled left and right lateral moraine with a lake in between and (c) glacial till exposed in a road cut (d) with striated sandstone clasts.

4.2 ^{36}Cl exposure ages

We collected a total of 20 glacial boulder samples from Velež and Crvanj mountains for ^{36}Cl cosmogenic nuclide dating purposes (Table 1). The sampled moraines belong to a group of the lowest moraines in both study areas and therefore mark the largest extent of palaeoglaciers that can be recognised on the basis of geomorphological evidence.

Denudation rates of carbonate rocks can be very high and are believed to increase with increasing MAP (Levenson et al., 2017; Ryb et al., 2014). The data from several carbonate terrains around the world show denudation rates of the order of 40 (± 20) mm ka^{-1} for areas with mean annual precipitation similar to that of Nevesinje (Levenson et al., 2017), while similar denudation rates (30-60 mm ka^{-1}) were recently measured also in the Mediterranean karst (SE France) (Thomas et al., 2018) independently of the precipitation amount. Thus, 40 mm ka^{-1} was used as the most representative erosion rate for the correction of all sample ages in this study.

Reported age uncertainties were given at the 1-sigma level (i.e., one standard deviation), which include both the analytical and production rate errors. The cosmogenic ages of boulders, and thus the age of moraines represent the beginning of glacier retreat i.e., change in the equilibrium conditions of the glacier mass, or stationing of the glacier on a terminal point.

4.2.1 Velež Mountain glacial chronology

Ten samples (Figure 6) were collected from the crest of one of the largest and best developed lateral-terminal moraine complexes on the Velež Mountain, located in the Budijevača Valley (Figures 2b, 7a and 7b). The sampled lateral-terminal moraine complex on Velež appears at 1300 m asl and after 2.7 km terminates at 980 m asl. It rises up to 130 m above the lake, which is located in between the moraine complex. The lithology of all boulders that were collected from this moraine complex is limestone, showing high concentrations of CaO (~55%) and very low K_2O and Cl (12.9-37.5 ppm), thus the main production mechanism (>95%) is spallation of Ca (Table 2, and supplementary Table S1).

Five boulders from the right lateral moraine of Budijevača Valley yielded ^{36}Cl ages of 14.1 ± 1.8 ka (BU16-01), 7.8 ± 0.9 ka (BU16-02), 10.9 ± 1.4 ka (BU16-03), 8.8 ± 1.1 ka (BU16-04) and 9.0 ± 1.0 ka (BU16-05). Boulders from the left lateral moraine gave ages of 15.7 ± 2.1 ka (BU16-06), 9.0 ± 1.0 ka (BU16-07), 6.3 ± 0.6 ka (BU16-08), 10.7 ± 1.3 ka (BU16-09) and 11.5 ± 1.4 ka (BU16-10) (Table 3).

Figure 6: Photos of the sampled boulders and their cosmogenic ages based on 40 mm ka-1 bedrock erosion rates on the Velež Mountain.

None of the measured ages is more than twice the standard deviation away from the mean of the surface exposure ages in a data set (Figure 8); therefore, no statistical outliers can be identified. However, the biggest and tallest two boulders (BU16-01, BU16-06) gave the oldest ages (14.1 ± 1.8 ka and 15.7 ± 2.1 ka, respectively) among the group of samples taken from this moraine complex,

408 which indicates the exhumation caused by erosion of the moraines is likely to have a great influence
409 on the age of samples. Assuming that inheritance is not a relevant process due to the position and
410 characteristics of the moraine, then the oldest ages are likely to best estimate the true depositional
411 age.

412 Therefore, the oldest two samples representing the best estimate of the age of the landform, give
413 ages of 14.1 ± 1.8 ka (BU16-01) for the right lateral moraine and 15.7 ± 2.1 (BU16-06) for the left
414 lateral moraine. These average ages of 14.9 ± 1.1 ka indicate the Oldest Dryas glaciation in the Velež
415 Mountain.

416

417 Figure 7: (a) GoogleEarth image and (b) an aerial photo of the Budijevača lateral-terminal moraine
418 complex. Sampling locations are marked with yellow points in (a), white dotted lines in (b) are
419 moraine crests and blue arrowed line is the direction of the glacier flow. Note the height (130 m) of
420 the moraine in (b).

421

422 Figure 8: Cosmogenic ^{36}Cl ages of the boulders from right- (RL) and left-lateral (LL) moraines of (a)
423 Mt. Velež and (b) Mt. Crvanj. Upper panels show the individual sample ages with 1-sigma
424 uncertainties, and the lower panels show the probably density functions (PDF) of the samples.
425 Average age of the oldest two samples (indicated by thick black PDF curves) from both data sets
426 were shown and assigned to the age of the landforms.

427

428 4.2.2 Crvanj Mountain glacial chronology

429 We also collected 10 samples (Figure 9) from a pair of lateral moraines on the western slopes of the
430 Crvanj Mountain (Figure 4b). The sampled pair of lateral moraines stretches between 1350 and 1120
431 m asl and stands approximately 150 m above the lake area. Boulders are of different carbonate
432 lithologies with prevailing seven dolostone and three limestone boulders. Dolostone samples

433 (samples from CR16-01 to CR16-06 and sample CR16-08) have lower concentrations of CaO (26.51-
434 43.59%), but much higher concentrations of Cl (155.7-450.0 ppm) compared to limestone samples
435 (samples CR16-07, 09 and 10) (Table 2), which make the low energy neutron capture reactions via
436 ^{35}Cl an important part of the production mechanism of ^{36}Cl (about 40% of total ^{36}Cl production)
437 (supplementary Table S1).

438 Six boulders were collected from the left lateral moraine that yield ages of 8.2 ± 1.6 ka (CR16-01), 9.2
439 ± 1.6 ka (CR16-02), 4.2 ± 1.0 ka (CR16-03), 8.4 ± 1.5 ka (CR16-04), 11.3 ± 2.5 ka (CR16-05) and 7.0 ±
440 1.2 ka (CR16-06) (Table 3). The samples taken from the right lateral moraine yielded slightly younger
441 ages, i.e. 7.0 ± 0.7 ka (CR16-07), 8.5 ± 1.4 ka (CR16-08), 8.3 ± 1.0 ka (CR16-09) and 12.4 ± 1.6 ka
442 (CR16-10).

443 Even in this data set the statistical outliers do not appear (Figure 8) and the largest and at the same
444 time the tallest boulder (CR16-05) gave the oldest age. We applied the same approach as for Velež
445 and chose the oldest sample from each lateral moraine as the most representative time of moraine
446 emplacement. The oldest two samples yielded ages of 11.3 ± 2.5 ka (CR16-05) for the left lateral
447 moraine and 12.4 ± 1.6 ka (CR16-10) for the right lateral moraine. The average age of two samples
448 (11.9 ± 0.8 ka) indicate the Younger Dryas stadial event in the Crvanj Mountain.

449

450 Table 3: Cosmogenic ^{36}Cl inventories, production rates, ages of boulders considering different erosion
451 rates and ages of glacial landforms using 40 mm ka^{-1} of erosion in the Velež and Crvanj mountains.

452

453 Figure 9: Photos of the sampled boulders and their cosmogenic ages on the Crvanj Mountain.

454

455 4.3 Palaeoglacier geometry

456 On the basis of additional field observations, we revised the palaeoglacier extent and ELA estimation
457 for the Velež Mountain, which have been previously presented by Žebre and Stepišnik (2015a).

458 However, the reconstruction of glaciers and ELAs on the Crvanj Mountain is presented for the first
459 time in this paper.

460 Geomorphological evidence indicates that during the maximum phase of glaciation the Velež glaciers
461 covered an area of approximately 28.2 km^2 (Figure 10a). The north-facing glaciers, to some extent
462 described already by Grund (1910, 1902), initiated in cirques, moved down the valleys and
463 terminated in the karst depressions north of the mountain. Eight km-wide and up to 210-m-thick
464 system of 7 interconnected valley glaciers, with a number of nunataks protruding above the ice
465 (Figure 10b and 10c), was situated below the cirque complex. Only two valley glaciers on the north-
466 facing slopes, the eastern- and westernmost ones, were disconnected from this uniform ice mass.
467 The lengths of the north-facing glaciers were between 1.5 and 5 km. The westernmost valley glacier
468 was the lowest glacier in the study area, which terminated at an altitude of 940 m asl. According to
469 the calculations made by Profiler v.2 (Benn and Hulton, 2010) the thicknesses of the ice below the
470 cirques were between 130 and 210 m. On the south-facing slopes below the highest peak Botin, only
471 two small cirque glaciers existed, covering an overall area of less than 1 km^2.

472

473 Figure 10: (a) Palaeoglacier geometry with 50 m glacier contour lines, (b) glacier extent with
474 longitudinal profiles used in glacier reconstruction, and (c) the modelled ice thickness of the Velež
475 glaciers. Numbers in (b) indicate separate valley and cirque glaciers used for the ELA calculations. For
476 the geomorphology and sampling locations refer to Figure 2a.
477

478 The Crvanj Mountain hosted a small ice field and two cirque glaciers with an overall area of 23.9 km^2
479 during the maximum phase of glaciation (Figure 11a). Four outlet glaciers, heading towards N, E and
480 S directions (Figure 11b), drained the ice field. The outlet glaciers were between 2 and 3.5 km long
481 and up to 1.5 km wide. They ended at elevations between 900 and 1200 m. The northern outlet
482 glacier might have reached lower altitudes, but owing to landmines in that area we were not able to

make the geomorphological investigation. The greatest ice thickness was calculated on the plateau area, reaching approximately 200 m (Figure 11c). The two cirque glaciers formed on the northwest-facing slopes and covered an area of 1.4 km^2.

Figure 11: (a) Palaeoglacier geometry with 50 m glacier contour lines, (b) glacier extent with longitudinal profiles used in glacier reconstruction, and (c) the modelled ice thickness of the Crvanj ice field. Numbers in (b) indicate separate outlet and cirque glaciers used for the ELA calculations. For the geomorphology and sampling locations refer to Figure 4a.

4.4 Palaeo-equilibrium line altitudes

The mean ELA of palaeoglaciers on the Velež Mountain was calculated to 1388 m (σ=186) using the BR ratio of 1.9 ± 0.81 (Rea, 2009) (Table 4). While the mean ELA of the north-facing valley glaciers was 1292 m, on the south-facing slopes where only two cirque glaciers formed, the ELA was 434 m higher. Applying the same BR ratio, the mean palaeo-ELA on the Crvanj Mountain was found at 1541 m (σ=46) (Table 4). The ELA of the ice field with pertaining outlet glaciers was calculated to 1476 m, while the ELA of cirque glaciers was 104 m higher. Northeast oriented glaciers had in general lower ELAs, which is reasonable owing to differences in solar radiation and temperatures between north and south facing slopes. However, the NE-SW difference in ELA is approximately 8-times higher on Velež (NE-SW ELA difference=434 m) compared to Crvanj (NE-SW ELA difference=52 m), which can be explained by different morpho-climatological conditions. The morphology of the Velež Mountain with steep north-facing slopes allowed the formation of valley glaciers, where the accumulation was likely dominated by windblown deposition and avalanches. These two mechanisms were not as pronounced on the Crvanj Mountain due to the ice field type glaciation and consequently the local ELA differences were relatively small.

To crosscheck the ELA calculations using the AABR method, we also applied the AAR method using the ratio of 0.6 (Benn and Evans, 1998; Nesje and Dahl, 2000; Porter, 1977), which is the most widely accepted, but not necessarily one of the most accurate methods (and ratios) for the palaeo-ELA calculations (e.g. Kern and László, 2010). The results differ insignificantly, since the mean ELA for the Velež Mountain is calculated to 1392 m and for the Crvanj Mountain to 1596 m. Taking into account the ELAs calculated with the AABR method, the Velež Mountain ELA is 153 m lower than the ELA on the Crvanj Mountain and 204 m lower in the case of AAR method.

Table 4: The estimated palaeoELAs (in metres) for all reconstructed palaeoglaciers on the Velež and Crvanj mountains (see Figure 10b and 11b for the location of each glacier). The applied method is area altitude balance ratio (AABR) with a ratio of 1.9 ± 0.81, which is representative for mid-latitude maritime glaciers according to empirically derived results by Rea (2009).

4.5 Degree-day model outputs

Because snowmelt equals snow accumulation at the ELA under equilibrium conditions, our melt predictions using a simple degree-day model show the amount of accumulation required to sustain the reconstructed glaciers (Table 5). Hypothesizing the existence of glaciers with the reconstructed ELAs on the Velež and Crvanj mountains in the recent climate, the annual accumulation required to offset melting would need to be 9304 and 8295 mm of water equivalent, respectively. Further hypothesizing the accumulation on palaeoglaciers was similar to the modern MAP at Nevesinje and the modern annual temperature range was same as today, then the temperature depression between 9 and 10 °C for Velež and between 8 and 9 °C for Crvanj is required to sustain the palaeoglaciers with reconstructed ELAs. This is a very rough estimation because annual accumulation on glacier approximates winter and not annual precipitation, excluding local inputs from avalanching and wind-blown snow. The Velež glaciers on the north-facing slopes were likely influenced by the

aforementioned local inputs, which makes the melt predictions further overestimated. If assuming higher annual temperature range because of possibly more continental climate during glacial stages, even higher accumulation is required to balance melting.

Table 5: The degree-day model outputs for the Velež and Crvanj palaeoglaciers based on the reconstructed mean ELAs for each mountain (ELA Velež =1388 m, ELA Crvanj=1541 m) and modern climate data from Nevesinje (891 m asl) (mean annual temperature=8.6 °C, mean annual temperature range=18.9 °C, MAP=1795 mm) for the period 1961-1990 (Data courtesy Federal Hydrometeorological Institute, Sarajevo).

5. Discussion

5.1 ^{36}Cl cosmogenic nuclide dating uncertainties

Apart from analytical and production rate uncertainties, geological uncertainties also have to be considered when interpreting exposure ages. The latter often overshadow the first two and are principally subject to prior-exposure (inheritance), reworking and exhumation of boulders on moraines and erosion rates. Influence of vegetation and snow cover as well as tectonic movements and other geomorphological processes can also play an important role in the interpretation of exposure ages. Below, we discuss in detail the most relevant uncertainties for our study area.

5.1.1 Moraine degradation and exhumation of boulders

Although moraines in karst areas dating to Last Glaciation but also to older Pleistocene glaciations (e.g. Hughes et al., 2011, 2010) are believed to be well-preserved because of the absence or minimal fluvial reworking, they nevertheless degrade due to karst denudation and the topography is getting smoother over time. Moraine crest lowering is more pronounced in its early stage, within the first few thousands of years after the moraine deposition, when majority of large boulders are exhumed (Putkonen and Swanson, 2003). However, there is a substantial difference in the intensity of

557 degradation among different types of moraines. Moraines with broad and flat crests, such as
558 hummocky moraines, will degrade less than for example lateral moraines with sharp crests and steep
559 slopes (Applegate et al., 2010; Putkonen and Swanson, 2003). In our case, the dated lateral moraines
560 exhibit smooth crest morphology and few large boulders are present on their crests. This indicates
561 that their post-glacial evolution has been influenced by a relatively marked degradation. Several
562 studies highlighted the problems related to the degradation of moraines and consequently the
563 boulder exhumation, resulting in cosmogenic ages that are inconsistent with the stratigraphic order
564 of moraines (e.g. Hughes et al., 2018; Palacios et al., 2019; Roy et al., 2017; Schaefer et al., 2008). The
565 influence of exhumation is particularly evident when trying to date moraine boulders older than Late
566 Pleistocene (Hughes et al., 2018). According to the moraine degradation model (Applegate et al.,
567 2010; Putkonen and Swanson, 2003), our dated moraines are supposed to degrade in the order of
568 ~20 m since Lateglacial. Our exposure ages likely reflect a range of ages when the active degradation
569 of the surface took place, and therefore in high precipitation regions we prefer to consider the oldest
570 age within a group as the best estimation of the true depositional age. Without erosion corrections,
571 these figures are 10.5 ± 0.9 ka for the Velež, and 15.6 ± 2.3 ka for the Crvanj mountains. The oldest
572 age in both cases is represented by the tallest and overall largest boulder within the group of
573 samples, which further demonstrates that the exhumation of boulders is one of the main geological
574 uncertainties to be considered while interpreting exposure ages in similar environments. This is in
575 accordance with the analysis of a large dataset of glacial boulders, confirming that tall boulders, most
576 likely with minimum post-glacial shielding, yield higher quality exposure ages (Heyman et al., 2016).

577 5.1.2 Inheritance

578 The inheritance is the initial nuclide concentration that is already in the rock before the beginning of
579 the final exposure (Ivy-Ochs and Schaller, 2009). Therefore, one of the most important assumptions
580 of the cosmogenic surface exposure dating is that the inheritance is negligible or could be
581 determined (Schmidt et al., 2011). Several studies related to moraine boulder inheritance indicate

582 that the glacier scouring of the bedrock is a very efficient mechanism in removing the pre-existing
583 cosmogenic component (e.g. Applegate et al., 2012, 2010; Davis et al., 1999; Dortch et al., 2013;
584 Hallet and Putkonen, 1994; Heyman et al., 2011). Several studies carried out on the moraine
585 boulders in the Taurus Mountain Range of Turkey since 2008 were compiled by Çiner et al. (2017)
586 (their figure 11), who concluded that out of 183 limestone samples, only 6 boulders (3.3%) were
587 outliers attributed to inheritance; the authors hence assumed this figure close to negligible. Although
588 few cases where inheritance is reported from moraine boulders (e.g. Dortch et al., 2013), we believe
589 that given the high erosion rates of the boulders, mainly due to high precipitation in our study area,
590 any inheritance related to prior exposure would have been zeroed. We therefore neglected
591 inheritance as a factor in our age calculations.

592 5.1.3 Karst denudation rate

593 In karst terrains, both chemical denudation and mechanical erosion processes operate and the total
594 karst denudation rate is the sum of both processes (Ford and Williams, 2007). Chemical denudation
595 rates established within karst vary due to runoff of precipitates, temperature and partial pressure of
596 carbon dioxide in surrounding atmospheres (Gunn, 2004). The chemical denudation rates are
597 regularly calculated through monitoring of dissolved mater content in karst springs (Ford and
598 Williams, 2007; Veress, 2009). Those values are non-relevant for determining karst denudation rates
599 on exposed carbonate bedrock (e.g. karren, glacial boulders), since there is no effect of enhanced
600 dissolution in epikarst subsoil environments. Relevant methods for exposed carbonate surfaces
601 include continual in-situ measurements by means of micro-erosion meter (Cucchi et al., 1995; Furlani
602 et al., 2009; Veress, 2009). However, these are only relevant for the recent climatic conditions.
603 Results from the northern part of the Dinaric Mountains highlight significant differences, which are
604 the result of lithological control coupled with climatic setting (Furlani et al., 2009). There are
605 differences between dolomites and calcarenites (~10 mm ka^{-1}) and micritic limestones (~40 mm ka^{-1})
606 (Cucchi et al., 1995; Furlani et al., 2009). Substantial differentiations in denudation rates are a

607 consequence of climatic setting and even small climatic variations (Mediterranean and sub-alpine
608 climate) can yield double denudation rates (Furlani et al., 2009). There is a shortage of detail
609 monitoring of micro-erosion meter denudation rates in high Dinaric environments. Available data
610 from the nearby Julian Alps on micritic limestones show average denudation rate of ~40 mm ka^{-1} with
611 considerable increases (up to ~100 mm ka^{-1}) within depressions with thicker snow cover (Kunaver,
612 1979). Those results correspond, in the order of magnitude, with other values obtained with the
613 same method in similar environments (Forti, 1984; Pulina, 1974). Furthermore, recently applied
614 measurements of ^{36}Cl concentrations for establishing denudation rates in different karst terrains
615 around the world (Levenson et al., 2017) and in SE France (Thomas et al., 2018) show denudation
616 rates in the order of 40±20 mm ka^{-1}. According to Thomas et al. (2018) there is no clear connection
617 between climatic spatial gradients and denudation rates; the latter are rather influenced by the
618 surface inclination. On the Velež and Crvanj mountains we deducted denudation rate at 40 mm ka^{-1}
619 even though previous researchers in the Balkans did not apply denudation corrections in cosmogenic
620 dating (Pope et al., 2015) or used rather low rates as 5 mm ka^{-1} (e.g. Gromig et al., 2018; Styllas et al.,
621 2018) (Table 6).

622

623 Table 6: A list of different dating methods applied to glacial landforms in the Balkan Peninsula. Note
624 that calculations of ^{36}Cl cosmogenic exposure ages from Mount Chelmos and Mount Olympus are
625 based on the production rates from Stone et al. (1996) and Schimmelpfennig et al. (2011),
626 respectively. For comparison, two boulder-ages from Mount Chelmos (CH10 (11.03 ± 0.9 ka), CH11
627 (8.76 ± 0.70 ka)) (Pope et al., 2015) and two boulder-ages from Mount Olympus (TZ03 (12.44 ± 1.07
628 ka), MK12 (12.37 ± 1.07 ka)) (Styllas et al., 2018) were recalculated using the production rates of
629 Marrero et al. (2016b). The two ages from Mount Olympus were also corrected for snow and
630 erosion, using the same values as in the paper of Styllas et al. (2018). The recalculated ages are 13-
631 14% younger for Mount Chelmos and 23-24% younger for Mount Olympus with respect to the

632 published ages. ^{14}C ages from Snežnik were recalculated according to the IntCal13 calibration
633 (Reimer et al., 2013). Recalculated ages are marked with asterisk.

634

635 5.1.4 Shielding

636 Post-depositional processes such as shielding by snow, vegetation, sediment and soil can reduce
637 nuclide concentrations on boulders, resulting in underestimation of landform ages. Although most
638 studies on moraines indicate that snow cover is a second-order process (~10% or less) (Schildgen et
639 al., 2005), a relatively thick snow cover might have been present in our study area because of high
640 precipitation potentials. As Velež and Crvanj mountains are geographically close, we assumed
641 identical snow shielding acting on the sampled boulders. We estimated a snowpack of 25, 100, 100,
642 100, 50, 25 cm of snow on Nov, Dec, Jan, Feb, Mar and Apr on top of boulders and calculated that
643 the total effect of snow correction of our samples to be around 4.9% (i.e. snow correction make the
644 ages 4.9% older). Doubling the snowpack data would add another 5.4% in average.

645 Another shielding factor might be related to vegetation. The presence of forest increases boulder
646 instability in matrix-rich moraines. Trees, soil and leaf litter decrease the cosmic rays reaching the
647 rock by only a few percent (Kubik et al., 1998). However, as trees grow or fall even large boulders can
648 be toppled (cf. Cerling and Craig, 1994). Assuming that dense trees covered the study areas, as we
649 see today, one would need to consider the shielding due to the vegetation during the exposure time
650 of the boulders.

651 5.2 Interpretation of ^{36}Cl cosmogenic nuclide dating results from the Velež and Crvanj mountains

652 After taking into account all relevant cosmogenic nuclide dating uncertainties for both study areas,
653 the most probable age of the dated moraines is Lateglacial, spanning from Oldest Dryas for Velež
654 (14.9 ± 1.1 ka) to Younger Dryas for Crvanj (11.9 ± 0.9 ka). These are still to be considered as

minimum ages. To better understand a relevance of the obtained ages, these have been put into the geomorphological and climate context.

According to the geomorphological evidence, the dated moraines mark the largest extent of glaciers in both study areas. These have been estimated to approximately 28 km^2 for Velež and 24 km^2 for Crvanj using field evidence combined with the glacier flow-line model. The ELAs have been calculated to 1388 m for Velež and 1541 m for Crvanj by applying the AABR method. Glaciers of similar size with so low ELAs during Younger or Oldest Dryas have not been reported until now for the Balkan Peninsula; they have been recorded only in the form of cirque glaciers (e.g. Gromig et al., 2018; Hughes et al., 2011, 2010; Kuhlemann et al., 2009; Pope et al., 2015; Ribolini et al., 2011, 2018; Styllas et al., 2018). Smaller moraines that are present at higher altitudes compared to the dated moraines in our study area (Figures 2 and 4) are in better agreement with the above-cited Lateglacial moraines and their corresponding ELAs. We would also assume that the dated moraines on both mountains pertain to the same glacial period, because they mark the largest extent of glaciers in their respective areas, which were of similar size. These local differences in ages might result from different denudation rates between dolostone and limestone lithologies, the first being dominant in the Crvanj area and the last in the Velež area (supplementary Table S1). Moreover, it would be unrealistic to assume that all LGM moraines would have been washed away or entirely degraded, also because moraines in karst environments generally tend to be better preserved compared to moraines in the typical alpine environments, where slope and fluvial processes are much more intense. Thus, it is difficult to justify the Lateglacial age of the reconstructed glaciers on Velež and Crvanj from the geomorphological context.

Temperature depressions between 8 and 10 °C are required to sustain the reconstructed glaciers with pertaining ELAs according to the degree-day model simulations (Table 5) if considering the accumulation on palaeoglaciers was similar or less than the modern MAP. This is in accordance with the reconstructed LGM temperature drop inferred from pollen for northern Greece and central Italy

(Peyron et al., 1998) as well as from ELAs for the Central Dinaric Mountains (Kuhlemann et al., 2008). Though some of the reported temperature depressions for the Oldest and Younger Dryas in the Balkan Peninsula are even more pronounced from those at LGM, like for example pollen inferred 10-14°C drop in temperature for Oldest Dryas and around 10°C for Younger Dryas in the Lake Maliq in Albania (Bordon et al., 2009). This is highly unlikely, also because no such drop in temperature has been confirmed elsewhere in the Mediterranean, while the Younger Dryas temperature depression inferred from the distribution of relict rock glaciers in the SE European Alps has been estimated to 3-4°C (Frauenfelder et al., 2001). MAAT depression of 4°C for Velež and Crvanj would result in 4807-5601 mm of water equivalent (w.e.) of annual melt at ELA, which is unrealistic. However, a drop in temperature of 5-6°C, which would result in 4064-4807 mm w.e. of snow accumulation required to balance melting at the ELAs of the reconstructed glaciers (Table 5), might be reasonable. The modern glaciers in the Pacific Coast Range with maritime climate (e.g. South Cascade glacier) having very high winter mass balance (~2000-4000 mm w.e.) and MAAT at the ELA close to or even above 0°C (Krimmel, 2001; Ohmura et al., 1992; WGMS, 2016), are good modern analogues to our reconstructed glaciers. Nevertheless, having glaciers in the Velež and Crvanj mountains with similar winter mass balance as today in the Pacific Coast Range would require substantially higher MAP than today.

The boulder ages reflect complex exhumation and denudation history, which at this point do not allow obtaining more precise moraine chronologies for the Velež and Crvanj mountains. Future work is needed to better understand the exhumation and denudation processes and their influence on the cosmogenic exposure dating approach in a karst landscape like the Dinaric Mountains. Both study areas as well as the entire country of Bosnia and Herzegovina lack any previous knowledge on the timing of glaciations, which makes the correlation of the age data very difficult. This is however a new dataset and presents a relevant contribution towards better understanding of the glacial chronologies in the Dinaric Mountains.

5.3 Glacial chronologies in the Balkans and elsewhere in the Mediterranean

Although the mountains in the Dinarides and elsewhere in the Balkan Peninsula exhibit large areas of glacially modified landscape, they are still poorly represented by age data, which makes a robust comparison with the Velež and Crvanj data rather difficult. The closest area with established glacial chronologies are mountains of Montenegro (Hughes et al., 2011, 2010) (Table 6, Figure 12), where Younger Dryas has been recorded only in the form of cirque glaciers, having ELA at 1465 m on the coastal Orjen Mountain. More distant Balkan areas with existent glacial chronologies, but still relevant for comparison with the Velež and Crvanj mountains, are the Šar Planina and Galičica mountains in the Former Yugoslav Republic of Macedonia (FYROM), and Mount Chelmos and Mount Olympus in Greece. The glacier advance in the course of Younger Dryas on the aforementioned mountains is also reported as cirque glaciations, with ELAs of 2300-2400 m on the Šar Planina Mountains (Kuhlemann et al., 2009), 2130 m on the Galičica Mountain (Gromig et al., 2018; Ribolini et al., 2011) and 2114 m on Mount Chelmos (Pope et al., 2015). ELA for Mount Olympus was estimated to 2200-2600 m for the LG1-3 Lateglacial phase, which corresponds to Younger Dryas period after the recalculation of the ages using the same production rates as those applied to our moraine boulders (Table 6). All the above-mentioned published ELAs have been recalculated (supplementary Table S2) to the same ELA method, and hence they are entirely comparable. The Younger Dryas advances in other Mediterranean mountains have been confirmed in the High Atlas (Hughes et al., 2018), Taurus Mountains (Sarıkaya and Çiner, 2017), Iberian Peninsula (Palacios et al., 2016) and Maritime Alps (Federici et al., 2017). While the Younger Dryas glaciers where restricted to cirque areas in the High Atlas, Taurus Mountains and majority of Iberia, they reached the size of short valley glaciers in the Central Pyrenees (García-Ruiz et al., 2016) and Maritime Alps (Federici et al., 2017). Nevertheless, the magnitude of glaciation on the Crvanj Mountain is outstanding when compared with other Younger Dryas glaciers in the Balkan Peninsula and elsewhere in the Mediterranean.

730 Glaciers in the Balkan Peninsula dated to the Oldest Dryas were as well small in extent, with ELAs
731 between 2200 and 2350 m on the Šar Planina Mountains (Kuhlemann et al., 2009), 2250 m on Mount
732 Pelister (Ribolini et al., 2018), and at 2000 m on the Galičica Mountain (Ribolini et al., 2011). The
733 Oldest Dryas advance on Orjen has not been recognized by Hughes et al. (2010), but from the
734 minimum ages provided by U-series dating that show early Holocene ages (Table 6), these can be
735 interpreted in terms of Younger Dryas (as interpreted by Hughes et al. (2010) or Oldest Dryas
736 glaciation with ELA at 1465 m. The calculated ELA for Velež is extremely low (1388 m) when
737 compared with the aforementioned ELAs, even after recalculating all the published ELAs
738 (supplementary Table S2). The Oldest Dryas advance in the Eastern Mediterranean has been
739 recognized on Dedegöl Mountains, where moraines were dated to between 16.4 ± 0.7 ka and 12.0 ±
740 1.0 ka (Köse et al., 2018), while Mt. Akdağ (14–17 ka), Mt. Sandıras (13–20 ka) and Erciyes Volcano
741 (14–17.5 ka) show similar Lateglacial chronologies (Sarıkaya and Çiner, 2017). Similar ages have also
742 been reported from other Mediterranean mountains (Federici et al., 2011; Palacios et al., 2016).

743 Several marine and continental proxies from the Adriatic Sea (e.g. Combourieu-Nebout et al., 2013;
744 Favaretto et al., 2008; Rossignol-Strick, 1995) and Balkan region (e.g. Aufgebauer et al., 2012; Bordon
745 et al., 2009; Vogel et al., 2010), respectively, indicate that the Younger Dryas and Oldest Dryas were
746 cold events. However, the relative amount and source of moisture is still a matter of debate. While
747 some argue for cold and dry glacier advance during Lateglacial (Ribolini et al., 2018; Styllas et al.,
748 2018), others suggest the climate at that time was humid (Hughes et al., 2011, 2010; Pope et al.,
749 2015). Thus, understanding palaeo-precipitation sources is of major importance for understanding
750 the zonal partitioning of glacier behaviour in the Balkan Peninsula. Pope et al. (2015) suggested that
751 the moisture bearing atmospheric systems delivering winter precipitation in the west central Balkan
752 Peninsula were different from those influencing southern Greece, the first being influenced by
753 cyclogenesis in the northern Adriatic (Hughes et al., 2010) whereas the latter likely received winter
754 precipitation from a western or southern source. The position of the polar jet stream is a key factor
755 in controlling precipitation pattern in the Mediterranean as well in the Balkan Peninsula. A general

idea of the southern shift of the polar jet stream during LGM, which brought a southward shift of the North Atlantic storm tracks to about 40°N (Hofer et al., 2012; Laîné et al., 2009), is well supported by atmospheric circulation models, but how the local synoptic circulation was acting in the Mediterranean area is still debatable. Recent findings suggest a southerly moisture transport across the southern Mediterranean and then approaching the Alps from southward direction (Luetscher et al., 2015), which is consistent with the idea of the moisture bearing atmospheric systems delivering high precipitation amount, mainly during spring and autumn, to the west central Balkans. While this precipitation pattern was suggested for the LGM, it might hold true also for the Younger Dryas and Oldest Dryas events, likely for a shorter period and not as intense as during LGM, but still supporting the idea, to some extent, of a relatively large ice masses on Velež and Crvanj during that time. Moreover, the Adriatic coast during LGM and Oldest Dryas was much further south with respect to the Younger Dryas (Figure 13a). This suggests that during Younger Dryas greater amount of moisture was available in the low-level jet, which is the main source for the orographic precipitation in the Dinaric Mountains. Even if temperatures at that time were not as low as during LGM, the available moisture might have been higher.

It is also worth noting the role of the orographic barrier of the Dinaric Mountains in capturing (today, and most likely also in the past) most of the humidity from the Adriatic Sea air masses, leaving the inland part of the Balkans relatively dry (Hughes et al., 2010). This effect is reflected in a strong west-east gradient in ELA, which was suggested for the last cold stage glaciers in Montenegro and Greece by Hughes et al. (2011, 2010, 2006). A rise in ELA of 100 m for every 15 km inland was calculated for the Montenegrin glaciers by the same authors. Similar pattern of the inland ELA rise can be recognized also for the Younger Dryas and Oldest Dryas glaciers in the part of the Balkan Peninsula facing the Adriatic Sea (Figure 12b and 12c), which suggests the west-east gradient in ELA was characteristic throughout the Late Pleistocene. We estimated a rise in the ELA of 94 m during the Younger Dryas and 77 m for the Oldest Dryas for every 15 km inland. Very low ELAs in our study areas seem to be shifted further inland (Figures 12b and 12c). This pattern might be related to the

782 fact that the first orographic barriers in the Neretva catchment are located more than 50 km from
783 the Adriatic coast and that specific topoclimatic conditions controlled the ELA depression. This might
784 be the reason why the Oldest Dryas ELA on Velež would have been lower than the ELA on Orjen,
785 since the modern MAP on Orjen is more than twice as high as on Velež.

786 On some of the massifs in the Iberian Peninsula the glaciers between 17.5 and 14.5 ka deposited
787 moraines that are spatially close to the LGM moraines (Palacios et al., 2016), which seem to be the
788 case also for some of the Turkish Mountains (e.g. Sarıkaya et al., 2014, 2009). However, in the Velež
789 and Crvanj mountains we did not find any geomorphological evidence that would imply larger glacier
790 extent, but closely spaced to the one we dated. It might be true that these large lateral-terminal
791 moraine complexes are products of several glacial stages, as has been already suggested by Žebre
792 and Stepišnik (2015a), which would imply that the glaciers on Velež and Crvanj reached their Late
793 Pleistocene maximum extents well after the global LGM. This is in agreement to some extent with
794 the ages obtained in the Šar Planina Mountain (Kuhlemann et al., 2009) and Montenegrin Mountains
795 (Hughes et al., 2011, 2010), where the moraines indicative for the local LGM were dated to the
796 period following the global LGM. The cosmogenic ages from terminal moraines in the Rila Mountain
797 (Kuhlemann et al., 2013) indicate that the local LGM extent occurred in two phases, i.e. prior and
798 after the global LGM. In contrast with the records in FYROM and Montenegro, the Late Pleistocene
799 glacier maximum on Mount Chelmos was dated to 40-30 ka and thus predates the global LGM (Pope
800 et al., 2015) (Table 6). While a relatively large LGM glaciation is reported from the Rila Mountains
801 (Kuhlemann et al., 2013), with 29 valley glaciers covering an area of 430 km^2 and having ELAs
802 between 2150 and 2290 m, from the Šar Planina Mountains with valley glaciers several km long
803 having ELAs between 1900 and 2300 m (Kuhlemann et al., 2009), and from Montenegro with several
804 smaller valley and cirque glaciers with a total area of 56 km^2 and ELAs between 1456 and 1952 m
805 (Hughes et al., 2011, 2010), much smaller glaciation in the form of cirque and small valley glaciers has
806 been recognized on Mount Chelmos (Pope et al., 2015), covering less than 5 km^2 in total, with the
807 mean ELA of 1986 m.

The evidence for older, Middle Pleistocene glaciations, when the glaciers in Montenegro, Greece and Croatia would have reached their maximum extent (Table 6), is missing in our study areas. It is obvious from several studies that the timing of glaciations not only varied across the Mediterranean mountains (Hughes and Woodward, 2017), but also on a regional scale across the Balkan Peninsula. Although our findings seem to match to a considerable extent to the results from the Balkan Peninsula and some other Mediterranean mountains, more research is needed in Bosnia and Herzegovina and in the Dinaric Mountains in general to better understand the climatic controls on glaciations and the asynchrony of glacier fluctuations amongst different areas. The focus of future research should be on moraine build-up during several glacial stages and possible age conflicts between different dating methods, as recently pointed out also by Rodríguez-Rodríguez et al. (2018).

Figure 12: (a) All locations in the Balkan Peninsula where moraines/outwash have been dated so far. Base layer of mountain belts is from https://ilias.unibe.ch/goto.php?target=file_1049915, based on the mountain definition by Kapos et al. (2000). Bathymetric data is from the European Marine Observation and Data Network (http://www.emodnet.eu/), while the sea level data for LGM, Oldest Dryas and Younger Dryas is from Lambeck et al. (2011). ELA as a function of the distance from the Adriatic Sea for (b) Younger Dryas and (b) Oldest Dryas. Only areas with absolute age data are taken into account.

6. Conclusions

The Velež and Crvanj mountains in the Dinaric mountain karst in Bosnia and Herzegovina were extensively glaciated during the Late Pleistocene despite their low altitude (<2000 m asl). During the most extensive glaciation total glacier area was 28.2 km^2 on the Velež Mountain and 23.9 km^2 on the Crvanj Mountain. High karst plateaux were covered by ice fields reaching thicknesses up to 200 m. Valley and outlet glaciers reached as far down as ~900 m asl, where large lateral-terminal moraine

complexes were deposited. Twenty glacial boulders from the largest two moraine complexes were sampled and dated using cosmogenic ^{36}Cl surface exposure dating. The obtained ages correspond to the Lateglacial advances, namely the Younger Dryas on Crvanj and the Oldest Dryas on Velež, although the age difference in the maximum glacier extent between the two mountains might result from different denudation rates. However, the magnitude of glaciation along with the equilibrium line altitude and degree day model simulations are exceptional in terms of the Lateglacial evidence in the Balkan Peninsula. A possible explanation for that might be an increased moisture supply during Lateglacial due to larger extent of the Adriatic Sea with respect to LGM along with specific topoclimatic conditions controlling the ELA depression. This paper presents the first attempt to date moraines in the Dinaric mountain karst using cosmogenic ^{36}Cl surface exposure dating and is thus an important contribution towards a better understanding of the timing of glaciations in the Dinaric Mountains. However, dating moraines in this type of karst with high precipitation amounts remains problematic owing mainly to unknown denudation rates and the magnitude of moraine degradation.

Acknowledgements

This work was supported by the Slovenian Research Agency (research core funding No. P1-0011 and P1-0025), The Scientific and Technological Research Council of Turkey (TÜBİTAK-118Y052) and the Istanbul Technical University Research Fund (project MGA-2017-40540). We are thankful to Klaus Wilcken at the ANSTO Lab in Australia for AMS measurements. We also acknowledge field assistance of Aleš Grlj (Institute of Anthropological and Spatial Studies, Slovenia) and laboratory assistance of Oğuzhan Köse (Istanbul Technical University). Nevesinje climate data are provided courtesy of the Federal Hydrometeorological Institute, Sarajevo, Federation of Bosnia and Herzegovina, Bosnia and Herzegovina. We also appreciate insightful comments and suggestions by Philip Hughes, Adriano Ribolini and one anonymous referee, which resulted in a much-improved manuscript.

857 **References**

858 Applegate, P.J., Urban, N.M., Keller, K., Lowell, T. V., Laabs, B.J.C., Kelly, M.A., Alley, R.B., 2012.
859 Improved moraine age interpretations through explicit matching of geomorphic process models
860 to cosmogenic nuclide measurements from single landforms. Quat. Res. 77, 293–304.
861 https://doi.org/10.1016/J.YQRES.2011.12.002

862 Applegate, P.J., Urban, N.M., Laabs, B.J.C., Keller, K., Alley, R.B., 2010. Model Development Modeling
863 the statistical distributions of cosmogenic exposure dates from moraines. Geosci. Model Dev. 3,
864 293–307.

865 Aufgebauer, A., Panagiotopoulos, K., Wagner, B., Schaebitz, F., Viehberg, F.A., Vogel, H., Zanchetta,
866 G., Sulpizio, R., Leng, M.J., Damaschke, M., 2012. Climate and environmental change in the
867 Balkans over the last 17 ka recorded in sediments from Lake Prespa (Albania/F.Y.R. of
868 Macedonia/Greece). Quat. Int. 274, 122–135. https://doi.org/10.1016/J.QUAINT.2012.02.015

869 Bavec, M., Tulaczyk, S.M., Mahan, S.A., Stock, G.M., 2004. Late Quaternary glaciation of the Upper
870 Soča River Region (Southern Julian Alps, NW Slovenia). Sediment. Geol. 165, 265–283.
871 https://doi.org/10.1016/j.sedgeo.2003.11.011

872 Benn, D.I., Evans, D.J.A., 1998. Glaciers and Glaciation. Edward Arnold, London.

873 Benn, D.I., Gemmell, A.M.D., 1997. Calculating equilibrium-line altitudes of former glaciers: a new
874 computer spreadsheet.

875 Benn, D.I., Hulton, N.R.J., 2010. An ExcelTM spreadsheet program for reconstructing the surface
876 profile of former mountain glaciers and ice caps. Comput. Geosci. 36, 605–610.
877 https://doi.org/10.1016/j.cageo.2009.09.016

878 Benn, D.I., Lehmkuhl, F., 2000. Mass balance and equilibrium-line altitudes of glaciers in high-
879 mountain environments. Quat. Int. 65–66, 15–29. https://doi.org/10.1016/S1040-

6182(99)00034-8

Bordon, A., Peyron, O., Lézine, A.-M., Brewer, S., Fouache, E., 2009. Pollen-inferred Late-Glacial and Holocene climate in southern Balkans (Lake Maliq). Quat. Int. 200, 19–30. https://doi.org/10.1016/J.QUAINT.2008.05.014

Braithwaite, R.J., 2008. Temperature and precipitation climate at the equilibrium-line altitude of glaciers expressed by the degree-day factor for melting snow. J. Glaciol. 54, 437–444. https://doi.org/10.3189/002214308785836968

Braithwaite, R.J., Raper, S.C.B., Chutko, K., 2006. Accumulation at the equilibrium-line altitude of glaciers inferred from a degree-day model and tested against field observations. Ann. Glaciol. 43, 329–334. https://doi.org/10.3189/172756406781812366

Brugger, K.A., 2006. Late Pleistocene climate inferred from the reconstruction of the Taylor River glacier complex, southern Sawatch Range, Colorado. Geomorphology 75, 318–329. https://doi.org/10.1016/J.GEOMORPH.2005.07.020

Cerling, T.E., Craig, H., 1994. Geomorphology and in-situ cosmogenic isotopes. Annu. Rev. Earth Planet. Sci. 22, 273–317.

Çiner, A., Sarıkaya, M.A., Yıldırım, C., 2017. Misleading old age on a young landform? The dilemma of cosmogenic inheritance in surface exposure dating: Moraines vs. rock glaciers. Quat. Geochronol. 42, 76–88. https://doi.org/10.1016/J.QUAGEO.2017.07.003

Combourieu-Nebout, N., Peyron, O., Bout-Roumazeilles, V., Goring, S., Dormoy, I., Joannin, S., Sadori, L., Siani, G., Magny, M., 2013. Holocene vegetation and climate changes in the central Mediterranean inferred from a high-resolution marine pollen record (Adriatic Sea). Clim. Past 9, 2023–2042. https://doi.org/10.5194/cp-9-2023-2013

Cowton, T., Hughes, P.D., Gibbard, P.L., 2009. Palaeoglaciation of Parque Natural Lago de Sanabria,

northwest Spain. Geomorphology 108, 282–291. https://doi.org/10.1016/J.GEOMORPH.2009.02.007

Cucchi, F., Forti, F., Marinetti, E., 1995. Surface degradation of carbonate rocks in the Karst of Trieste (Classical Karst, Italy), in: Formos, J.J., Ginés, A. (Eds.), Karren Landforms. Palma, pp. 41–51.

Cvijić, J., 1899. Glacijalne i morfološke studije o planinama Bosne, Hercegovine i Crne Gore. Državna štamparija Kraljevine Srbije, Beograd.

Davis, P.T., Bierman, P.R., Marsella, K.A., Caffee, M.W., Southon, J.R., 1999. Cosmogenic analysis of glacial terrains in the eastern Canadian Arctic: a test for inherited nuclides and the effectiveness of glacial erosion. Ann. Glaciol. 28, 181–188. https://doi.org/10.3189/172756499781821805

Davis, R., Schaeffer, O.A., 1955. Chlorine-36 in nature. Ann. N. Y. Acad. Sci. 62, 107–121. https://doi.org/https://doi.org/10.1111/j.1749-6632.1955.tb35368.x

Desilets, D., Zreda, M., Almasi, P.F., Elmore, D., 2006. Determination of cosmogenic 36Cl in rocks by isotope dilution: innovations, validation and error propagation. Chem. Geol. 233, 185–195. https://doi.org/10.1016/J.CHEMGEO.2006.03.001

Dortch, J.M., Owen, L.A., Caffee, M.W., 2013. Timing and climatic drivers for glaciation across semi-arid western Himalayan–Tibetan orogen. Quat. Sci. Rev. 78, 188–208. https://doi.org/10.1016/J.QUASCIREV.2013.07.025

Dunai, T., 2010. Cosmogenic Nuclides Principles, Concepts and Applications in the Earth Surface Sciences. Cambridge Academic Press.

Evans, D.J.A., Benn, D.I. (Eds.), 2004. A practical guide to the study of glacial sediments. Arnold, London.

Favaretto, S., Asioli, A., Miola, A., Piva, A., 2008. Preboreal climatic oscillations recorded by pollen and foraminifera in the southern Adriatic Sea. Quat. Int. 190, 89–102.

926 https://doi.org/https://doi.org/10.1016/j.quaint.2008.04.005

927 Federici, P.R., Granger, D.E., Ribolini, A., Spagnolo, M., Pappalardo, M., Cyr, A.J., 2011. Last Glacial
928 Maximum and the Gschnitz stadial in the Maritime Alps according to 10Be cosmogenic dating.
929 Boreas 41, 277–291. https://doi.org/10.1111/j.1502-3885.2011.00233.x

930 Federici, P.R., Ribolini, A., Spagnolo, M., 2017. Glacial history of the Maritime Alps from the Last
931 Glacial Maximum to the Little Ice Age. Geol. Soc. London, Spec. Publ. 433, 137–159.
932 https://doi.org/10.1144/SP433.9

933 Ford, D., Williams, P.D., 2007. Karst Hydrogeology and Geomorphology. Wiley, Chichester.

934 Forti, F., 1984. Messungen des Karstabtrages in der Region Friaul-Julisch-Venetien (Italien). Die Höhle
935 35, 135–139.

936 Frauenfelder, R., Haeberli, W., Hoelzle, M., Maisch, M., 2001. Using relict rockglaciers in GIS-based
937 modelling to reconstruct Younger Dryas permafrost distribution patterns in the Err-Julier area,
938 Swiss Alps. Nor. Geogr. Tidsskr. 55, 195–202. https://doi.org/10.1080/00291950152746522

939 Furlani, S., Cucchi, F., Forti, F., Rossi, A., 2009. Comparison between coastal and inland Karst
940 limestone lowering rates in the northeastern Adriatic Region (Italy and Croatia).
941 Geomorphology 104, 73–81. https://doi.org/10.1016/J.GEOMORPH.2008.05.015

942 Gachev, E., Stoyanov, K., Gikov, A., 2016. Small glaciers on the Balkan Peninsula: State and changes in
943 the last several years. Quat. Int. 415, 33–54. https://doi.org/10.1016/J.QUAINT.2015.10.042

944 García-Ruiz, J.M., Palacios, D., González-Sampériz, P., de Andrés, N., Moreno, A., Valero-Garcés, B.,
945 Gómez-Villar, A., 2016. Mountain glacier evolution in the Iberian Peninsula during the Younger
946 Dryas. Quat. Sci. Rev. 138, 16–30. https://doi.org/10.1016/J.QUASCIREV.2016.02.022

947 Gosse, J.C., Phillips, F.M., 2001. Terrestrial in situ cosmogenic nuclides: theory and application. Quat.
948 Sci. Rev. 20, 1475–1560. https://doi.org/10.1016/S0277-3791(00)00171-2

949 Gromig, R., Mechernich, S., Ribolini, A., Wagner, B., Zanchetta, G., Isola, I., Bini, M., Dunai, T.J., 2018.
950 Evidence for a Younger Dryas deglaciation in the Galicica Mountains (FYROM) from cosmogenic
951 36Cl. Quat. Int. 464, 352–363. https://doi.org/10.1016/j.quaint.2017.07.013

952 Grund, A., 1910. Beiträge zur Morphologie des Dinarischen Gebirges, in: Geographische
953 Abhandlungen. B. G. Teubner, Berlin, p. 230.

954 Grund, A., 1902. Neue Eiszeitspuren aus Bosnien und der Hercegovina. Globus 81, 149–150.

955 Gunn, J., 2004. Erosion rates: field measurements, in: Gunn, J. (Ed.), Encyclopedia of Caves and Karst
956 Science. Fitzroy Dearborn, New York, London, pp. 664–668.

957 Habič, P., 1968. Kraški svet med Idrijco in Vipavo. Slovenska akademija znanosti in umetnosti,
958 Ljubljana.

959 Hallet, B., Putkonen, J., 1994. Surface Dating of Dynamic Landforms: Young Boulders on Aging
960 Moraines. Science (80-.). 265, 937–940. https://doi.org/10.1126/science.265.5174.937

961 Heisinger, B., Lal, D., Jull, A.J.T., Kubik, P., Ivy-Ochs, S., Knie, K., Nolte, E., 2002. Production of selected
962 cosmogenic radionuclides by muons: 2. Capture of negative muons. Earth Planet. Sci. Lett. 200,
963 357–369. https://doi.org/10.1016/S0012-821X(02)00641-6

964 Heyman, J., Applegate, P.J., Blomdin, R., Gribenski, N., Harbor, J.M., Stroeven, A.P., 2016. Boulder
965 height – exposure age relationships from a global glacial 10Be compilation. Quat. Geochronol.
966 34, 1–11. https://doi.org/10.1016/J.QUAGEO.2016.03.002

967 Heyman, J., Stroeven, A.P., Harbor, J.M., Caffee, M.W., 2011. Too young or too old: Evaluating
968 cosmogenic exposure dating based on an analysis of compiled boulder exposure ages. Earth
969 Planet. Sci. Lett. 302, 71–80. https://doi.org/10.1016/J.EPSL.2010.11.040

970 Hofer, D., Raible, C.C., Merz, N., Dehnert, A., Kuhlemann, J., 2012. Simulated winter circulation types
971 in the North Atlantic and European region for preindustrial and glacial conditions. Geophys. Res.

Lett. 39. https://doi.org/10.1029/2012GL052296

Hrvatović, H., 2005. Geological guidebook through Bosnia and Herzegovina. Geological Survey of Federation of Bosnia and Herzegovina, Sarajevo.

Hughes, P.D., 2008. Response of a Montenegro glacier to extreme summer heatwaves in 2003 and 2007. Geogr. Ann. Ser. A, Phys. Geogr. 90, 259–267. https://doi.org/10.1111/j.1468-0459.2008.00344.x

Hughes, P.D., Fink, D., Rodés, Á., Fenton, C.R., Fujioka, T., 2018. Timing of Pleistocene glaciations in the High Atlas, Morocco: New 10Be and 36Cl exposure ages. Quat. Sci. Rev. 180, 193–213. https://doi.org/10.1016/J.QUASCIREV.2017.11.015

Hughes, P.D., Gibbard, P.L., Ehlers, J., 2013. Timing of glaciation during the last glacial cycle: evaluating the concept of a global 'Last Glacial Maximum' (LGM). Earth-Science Rev. 125, 171–198. https://doi.org/http://dx.doi.org/10.1016/j.earscirev.2013.07.003

Hughes, P.D., Woodward, J.C., 2017. Quaternary glaciation in the Mediterranean mountains: a new synthesis. Geol. Soc. London, Spec. Publ. 433, 1–23. https://doi.org/10.1144/SP433.14

Hughes, P.D., Woodward, J.C., Gibbard, P.L., Macklin, M.G., Gilmour, M.A., Smith, G.R., 2006. The Glacial History of the Pindus Mountains, Greece. J. Geol. 114, 413–434. https://doi.org/10.1086/504177

Hughes, P.D., Woodward, J.C., van Calsteren, P.C., Thomas, L.E., 2011. The glacial history of the Dinaric Alps, Montenegro. Quat. Sci. Rev. 30, 3393–3412. https://doi.org/10.1016/j.quascirev.2011.08.016

Hughes, P.D., Woodward, J.C., van Calsteren, P.C., Thomas, L.E., Adamson, K.R., 2010. Pleistocene ice caps on the coastal mountains of the Adriatic Sea. Quat. Sci. Rev. 29, 3690–3708. https://doi.org/10.1016/j.quascirev.2010.06.032

995 Ivy-Ochs, S., Schaller, M., 2009. Chapter 6 Examining Processes and Rates of Landscape Change with
996 Cosmogenic Radionuclides. Radioact. Environ. 16, 231–294. https://doi.org/10.1016/S1569-
997 4860(09)01606-4

998 Ivy-Ochs, S., Synal, H.-A., Roth, C., Schaller, M., 2004. Initial results from isotope dilution for Cl and
999 36Cl measurements at the PSI/ETH Zurich AMS facility. Nucl. Instruments Methods Phys. Res.
1000 Sect. B Beam Interact. with Mater. Atoms 223–224, 623–627.
1001 https://doi.org/10.1016/J.NIMB.2004.04.115

1002 Kapos, V., Rhind, J., Edwards, M., Price, M., Ravilious, C., 2000. Developing a map of the world's
1003 mountain forests, in: Price, M., Butt, N. (Eds.), Forests in Sustainable Mountain Development: A
1004 Report for 2000. CAB International, Wallingford, pp. 4–9. https://doi.org/10.1007/1-4020-3508-
1005 X_52

1006 Kern, Z., László, P., 2010. Size specific steady-state accumulation-area ratio: an improvement for
1007 equilibrium-line estimation of small palaeoglaciers. Quat. Sci. Rev. 29, 2781–2787.
1008 https://doi.org/10.1016/J.QUASCIREV.2010.06.033

1009 Köse, O., Sarıkaya, M.A., Çiner, A., Candaş, A., 2018. Late Quaternary glaciations and cosmogenic 36Cl
1010 geochronology of the Mount Dedegöl, SW Turkey. J. Quat. Sci. 33, 9,
1011 https://doi.org/10.1002/jqs.3080

1012 Kottek, M., Grieser, J., Beck, C., Rudolf, B., Rubel, F., 2006. World Map of the Köppen-Geiger climate
1013 classification updated. Meteorol. Zeitschrift 15, 259–263. https://doi.org/10.1127/0941-
1014 2948/2006/0130

1015 Krimmel, R.M., 2001. Water, Ice, Meteorological, and Speed Measurements at South Cascade
1016 Glacier, Washington,1999 Balance Year. U.S. Geological Survey, Tacoma, Washington.

1017 Krklec, K., Domínguez-Villar, D., Perica, D., 2015. Depositional environments and diagenesis of a

carbonate till from a Quaternary paleoglacier sequence in the Southern Velebit Mountain (Croatia). Palaeogeogr. Palaeoclimatol. Palaeoecol. 436, 188–198. https://doi.org/10.1016/J.PALAEO.2015.07.004

Kubik, P.W., Ivy-Ochs, S., Masarik, J., Frank, M., Schlüchter, C., 1998. 10Be and 26Al production rates deduced from an instantaneous event within the dendro-calibration curve, the landslide of Köfels, Ötz Valley, Austria. Earth Planet. Sci. Lett. 161, 231–241. https://doi.org/10.1016/S0012-821X(98)00153-8

Kuhlemann, J., Gachev, E., Gikov, A., Nedkov, S., Krumrei, I., Kubik, P., 2013. Glaciation in the Rila mountains (Bulgaria) during the Last Glacial Maximum. Quat. Int. 293, 51–62. https://doi.org/10.1016/J.QUAINT.2012.06.027

Kuhlemann, J., Milivojević, M., Krumrei, I., Kubik, P.W., 2009. Last glaciation of the Šara Range (Balkan peninsula): Increasing dryness from the LGM to the Holocene. Austrian J. Earth Sci. 102, 146–158.

Kuhlemann, J., Rohling, E.J., Krumrei, I., Kubik, P., Ivy-Ochs, S., Kucera, M., 2008. Regional Synthesis of Mediterranean Atmospheric Circulation During the Last Glacial Maximum. Science (80-.). 321, 1338–1340. https://doi.org/10.1126/science.1157638

Kunaver, J., 1979. Some experiences in measuring the surface karst denudation in high alpine environment, in: Actes Du Symposium International Sur l'érosion Karstique, Aix En Provence. pp. 75–85.

Laîné, A., Kageyama, M., Salas-Mélia, D., Voldoire, A., Rivière, G., Ramstein, G., Planton, S., Tyteca, S., Peterschmitt, J.Y., 2009. Northern hemisphere storm tracks during the last glacial maximum in the PMIP2 ocean-atmosphere coupled models: energetic study, seasonal cycle, precipitation. Clim. Dyn. 32, 593–614. https://doi.org/10.1007/s00382-008-0391-9

1041 Lambeck, K., Antonioli, F., Anzidei, M., Ferranti, L., Leoni, G., Scicchitano, G., Silenzi, S., 2011. Sea
1042 level change along the Italian coast during the Holocene and projections for the future. Quat.
1043 Int. 232, 250–257. https://doi.org/https://doi.org/10.1016/j.quaint.2010.04.026

1044 Levenson, Y., Ryb, U., Emmanuel, S., 2017. Comparison of field and laboratory weathering rates in
1045 carbonate rocks from an Eastern Mediterranean drainage basin. Earth Planet. Sci. Lett. 465,
1046 176–183. https://doi.org/10.1016/j.epsl.2017.02.031

1047 Lewin, J., Macklin, M.G., Woodward, J.C., 1991. Late quaternary fluvial sedimentation in the
1048 voidomatis basin, Epirus, Northwest Greece. Quat. Res. 35, 103–115.
1049 https://doi.org/https://doi.org/10.1016/0033-5894(91)90098-P

1050 Liedtke, V.H., 1962. Vergletscherungsspuren und Periglazialerscheinungen am Südhang des Lovcen
1051 östlich von Kotor. Eiszeitalter und Gegenwart 13, 15–18.

1052 Lifton, N., Sato, T., Dunai, T.J., 2014. Scaling in situ cosmogenic nuclide production rates using
1053 analytical approximations to atmospheric cosmic-ray fluxes. Earth Planet. Sci. Lett. 386, 149–
1054 160. https://doi.org/10.1016/J.EPSL.2013.10.052

1055 Luetscher, M., Boch, R., Sodemann, H., Spötl, C., Cheng, H., Edwards, R.L., Frisia, S., Hof, F., Müller,
1056 W., 2015. North Atlantic storm track changes during the Last Glacial Maximum recorded by
1057 Alpine speleothems. Nat. Commun. 6, 6344. https://doi.org/10.1038/ncomms7344

1058 Marjanac, L., 2012. Pleistocene glacial and periglacial sediments of Kvarner, northern Dalmatia and
1059 southern Velebit Mt. – evidence of Dinaric glaciation. PhD thesis. University of Zagreb.

1060 Marjanac, L., Marjanac, T., Mogut, K., 2001. Dolina Gumance u doba Pleistocena. Zb. Društva za Povj.
1061 Klana 6, 321–330.

1062 Marjanac, T., Marjanac, L., 2016. The extent of middle Pleistocene ice cap in the coastal Dinaric
1063 Mountains of Croatia. Quat. Res. 85, 445–455.

https://doi.org/https://doi.org/10.1016/j.yqres.2016.03.006

Marrero, S.M., Phillips, F.M., Borchers, B., Lifton, N., Aumer, R., Balco, G., 2016a. Cosmogenic nuclide systematics and the CRONUScalc program. Quat. Geochronol. 31, 160–187. https://doi.org/10.1016/j.quageo.2015.09.005

Marrero, S.M., Phillips, F.M., Caffee, M.W., Gosse, J.C., 2016b. CRONUS-Earth cosmogenic 36Cl calibration. Quat. Geochronol. 31, 199–219. https://doi.org/10.1016/j.quageo.2015.10.002

Milivojević, M., 2007. Glacijalni reljef na Volujaku sa Bioč em i Maglićem, in: Posebna Izdanja, Srpska Akademija Nauka i Umetnosti, Geografski Institut “Jovan Cvijić”, Knj. 68. Geografski institut “Jovan Cvijić” SANU, Beograd, p. 130.

Milivojević, M., Menković, L., Ćalić, J., 2008. Pleistocene glacial relief of the central part of Mt. Prokletije (Albanian Alps). Quat. Int. 190, 112–122. https://doi.org/10.1016/j.quaint.2008.04.006

Monegato, G., Ravazzi, C., Donegana, M., Pini, R., Calderoni, G., Wick, L., 2007. Evidence of a two-fold glacial advance during the last glacial maximum in the Tagliamento end moraine system (eastern Alps). Quat. Res. 68, 284–302. https://doi.org/10.1016/j.yqres.2007.07.002

Nesje, A., Dahl, S.O., 2000. Glaciers and environmental change. Arnold, London.

Nieuwendam, A., Ruiz-Fernández, J., Oliva, M., Lopes, V., Cruces, A., Conceição Freitas, M., 2016. Postglacial Landscape Changes and Cryogenic Processes in the Picos de Europa (Northern Spain) Reconstructed from Geomorphological Mapping and Microstructures on Quartz Grains. Permafr. Periglac. Process. 27, 96–108. https://doi.org/10.1002/ppp.1853

Ohmura, A., Kasser, P., Funk, M., 1992. Climate at the equilibrium line of glaciers. J. Glaciol.

Osmaston, H., 2005. Estimates of glacier equilibrium line altitudes by the Area×Altitude, the Area×Altitude Balance Ratio and the Area×Altitude Balance Index methods and their validation.

1087 Quat. Int. 138–139, 22–31. https://doi.org/https://doi.org/10.1016/j.quaint.2005.02.004

1088 Osnovna geološka karta (OGK) SFRJ. 1:100.000. List Kalinovik K 34-13 (Basic Geological Map of SFR
1089 Yugoslavia 1:100.000, Sheet Kalinovik K 34-13), 1981.

1090 Osnovna geološka karta (OGK) SFRJ. 1:100.000. List Mostar K 33-24 (Basic Geological Map of SFR
1091 Yugoslavia 1:100.000, Sheet Mostar K 33-24), 1970.

1092 Owen, L.A., Gualtieri, L., Finkel, R.C., Caffee, M.W., Benn, D.I., Sharma, M.C., 2001. Cosmogenic
1093 radionuclide dating of glacial landforms in the Lahul Himalaya, northern India: defining the
1094 timing of Late Quaternary glaciation. J. Quat. Sci. 16, 555–563. https://doi.org/10.1002/jqs.621

1095 Palacios, D., de Andrés, N., Gómez-Ortiz, A., García-Ruiz, J.M., 2016. Evidence of glacial activity during
1096 the Oldest Dryas in the mountains of Spain. Geol. Soc. London, Spec. Publ. 433.

1097 Palacios, D., Gómez-Ortiz, A., Alcalá-Reygosa, J., Andrés, N., Oliva, M., Tanarro, L.M., Salvador-Franch,
1098 F., Schimmelpfennig, I., Fernández-Fernández, J.M., Léanni, L., 2019. The challenging application
1099 of cosmogenic dating methods in residual glacial landforms: The case of Sierra Nevada (Spain).
1100 Geomorphology 325, 103–118.
1101 https://doi.org/https://doi.org/10.1016/j.geomorph.2018.10.006

1102 Pellitero, R., Rea, B.R., Spagnolo, M., Bakke, J., Hughes, P., Ivy-Ochs, S., Lukas, S., Ribolini, A., 2015. A
1103 GIS tool for automatic calculation of glacier equilibrium-line altitudes. Comput. Geosci. 82, 55–
1104 62. https://doi.org/10.1016/j.cageo.2015.05.005

1105 Pellitero, R., Rea, B.R., Spagnolo, M., Bakke, J., Ivy-Ochs, S., Frew, C.R., Hughes, P., Ribolini, A., Lukas,
1106 S., Renssen, H., 2016. GlaRe, a GIS tool to reconstruct the 3D surface of palaeoglaciers. Comput.
1107 Geosci. 94, 77–85. https://doi.org/10.1016/j.cageo.2016.06.008

1108 Penck, A., 1900. Die Eiszeitspuren auf der Balkanhalbinsel. Globus 78, 133–178.

1109 Petrović, A.S., 2014. A Reconstruction of the Pleistocene Glacial Maximum in the Žijovo Range

(Prokletije Mountains, Montenegro). Acta Geogr. Slov. 54, 256–269. https://doi.org/https://doi.org/10.3986/AGS54202

Peyron, O., Guiot, J., Cheddadi, R., Tarasov, P., Reille, M., de Beaulieu, J.-L., Bottema, S., Andrieu, V., 1998. Climatic Reconstruction in Europe for 18,000 YR B.P. from Pollen Data. Quat. Res. 49, 183–196. https://doi.org/10.1006/QRES.1997.1961

Pilaar Birch, S.E., Vander Linden, M., 2018. A long hard road… Reviewing the evidence for environmental change and population history in the eastern Adriatic and western Balkans during the Late Pleistocene and Early Holocene. Quat. Int. 465, 177–191. https://doi.org/10.1016/J.QUAINT.2016.12.035

Pope, R.J., Hughes, P.D., Skourtsos, E., 2015. Glacial history of Mt Chelmos, Peloponnesus, Greece. Geol. Soc. London, Spec. Publ. 433. https://doi.org/10.1144/SP433.11

Porter, S.C., 1977. Present and Past Glaciation Threshold in the Cascade Range, Washington, U.S.A.: Topographic and Climatic Controls, and Paleoclimatic Implications. J. Glaciol. 18, 101–116. https://doi.org/10.3189/S0022143000021559

Pulina, M., 1974. Denudacja chemiczna na obszarach krasu węglanowego = Chemical denudation on the carbonate karst areas. Polska akademia nauki, Institut geografii, Wroclaw.

Putkonen, J., Swanson, T., 2003. Accuracy of cosmogenic ages for moraines. Quat. Res. 59, 255–261. https://doi.org/10.1016/S0033-5894(03)00006-1

Rea, B.R., 2009. Defining modern day Area-Altitude Balance Ratios (AABRs) and their use in glacier-climate reconstructions. Quat. Sci. Rev. 28, 237–248. https://doi.org/10.1016/J.QUASCIREV.2008.10.011

Reimer, P.J., Bard, E., Bayliss, A., Beck, J.W., Blackwell, P.G., Bronk Ramsey, C., Buck, C.E., Cheng, H., Edwards, R.L., Friedrich, M., Grootes, P.M., Guilderson, T.P., Haflidason, H., Hajdas, I., Hatté, C.,

Heaton, T.J., Hoffmann, D.L., Hogg, A.G., Hughen, K.A., Kaiser, K.F., Kromer, B., Manning, S.W., Niu, M., Reimer, R.W., Richards, D.A., Scott, E.M., Southon, J.R., Staff, R.A., Turney, C.S.M., van der Plicht, J., 2013. IntCal13 and Marine13 Radiocarbon Age Calibration Curves 0–50,000 Years cal BP. Radiocarbon 55, 1869–1887. https://doi.org/10.2458/azu_js_rc.55.16947

Ribolini, A., Bini, M., Isola, I., Spagnolo, M., Zanchetta, G., Pellitero, R., Mechernich, S., Gromig, R., Dunai, T., Wagner, B., Milevski, I., 2018. An Oldest Dryas glacier expansion on Mount Pelister (Former Yugoslavian Republic of Macedonia) according to 10Be cosmogenic dating. J. Geol. Soc. London. 175, 100–110. https://doi.org/10.1144/jgs2017-038

Ribolini, A., Isola, I., Zanchetta, G., Bini, M., Sulpizio, R., 2011. Glacial features on the Galicica Mountains, Macedonia: Preliminary report. Geogr. Fis. e Din. Quat. 34, 247–255. https://doi.org/10.4461/GFDQ.2011.34.22

Riđanović, J., 1966. Orjen – La montagne dinarique. Radovi geografskog instituta sveučilišta u Zagrebu. Geografski institut, Prirodoslovno-matematički fakultet, Zagreb.

Rodríguez-Rodríguez, L., Domínguez-Cuesta, M.J., Rinterknecht, V., Jiménez-Sánchez, M., González-Lemos, S., Léanni, L., Sanjurjo, J., Ballesteros, D., Valenzuela, P., Llana-Fúnez, S., 2018. Constraining the age of superimposed glacial records in mountain environments with multiple dating methods (Cantabrian Mountains, Iberian Peninsula). Quat. Sci. Rev. 195, 215–231. https://doi.org/10.1016/J.QUASCIREV.2018.07.025

Rossignol-Strick, M., 1995. Sea-land correlation of pollen records in the Eastern Mediterranean for the glacial-interglacial transition: Biostratigraphy versus radiometric time-scale. Quat. Sci. Rev. 14, 893–915. https://doi.org/https://doi.org/10.1016/0277-3791(95)00070-4

Roy, M. Le, Deline, P., Carcaillet, J., Schimmelpfennig, I., Ermini, M., 2017. 10Be exposure dating of the timing of Neoglacial glacier advances in the Ecrins-Pelvoux massif, southern French Alps. Quat. Sci. Rev. 178, 118–138. https://doi.org/https://doi.org/10.1016/j.quascirev.2017.10.010

1157 Ruiz-Fernández, J., Oliva, M., Cruces, A., Lopes, V., Freitas, M. da C., Andrade, C., García-Hernández,
1158 C., López-Sáez, J.A., Geraldes, M., 2016. Environmental evolution in the Picos de Europa
1159 (Cantabrian Mountains, SW Europe) since the Last Glaciation. Quat. Sci. Rev. 138, 87–104.
1160 https://doi.org/10.1016/j.quascirev.2016.03.002

1161 Ryb, U., Matmon, A., Erel, Y., Haviv, I., Benedetti, L., Hidy, A.J., 2014. Styles and rates of long-term
1162 denudation in carbonate terrains under a Mediterranean to hyper-arid climatic gradient. Earth
1163 Planet. Sci. Lett. 406, 142–152. https://doi.org/10.1016/J.EPSL.2014.09.008

1164 Sarıkaya, M., Çiner, A., 2017. Late Quaternary glaciations in the eastern Mediterranean, in: Hughes,
1165 P., Woodward, J. (Eds.), Quaternary Glaciation in the Mediterranean Mountains. Geological
1166 Society of London Special Publication 433, pp. 289–305. https://doi.org/10.1144/SP433.4

1167 Sarıkaya, M.A., 2009. Late Quaternary glaciation and paleoclimate of Turkey inferred from
1168 cosmogenic 36Cl dating of moraines and glacier modeling. PhD thesis. University of Arizona,
1169 USA.

1170 Sarıkaya, M.A., Çiner, A., Haybat, H., Zreda, M., 2014. An early advance of glaciers on Mount Akdağ,
1171 SW Turkey, before the global Last Glacial Maximum; insights from cosmogenic nuclides and
1172 glacier modeling. Quat. Sci. Rev. 88, 96–109. https://doi.org/10.1016/J.QUASCIREV.2014.01.016

1173 Sarıkaya, M.A., Zreda, M., Çiner, A., 2009. Glaciations and paleoclimate of Mount Erciyes, central
1174 Turkey, since the Last Glacial Maximum, inferred from 36Cl cosmogenic dating and glacier
1175 modeling. Quat. Sci. Rev. 28, 2326–2341. https://doi.org/10.1016/J.QUASCIREV.2009.04.015

1176 Schaefer, J.M., Oberholzer, P., Zhao, Z., Ivy-Ochs, S., Wieler, R., Baur, H., Kubik, P.W., Schlüchter, C.,
1177 2008. Cosmogenic beryllium-10 and neon-21 dating of late Pleistocene glaciations in Nyalam,
1178 monsoonal Himalayas. Quat. Sci. Rev. 27, 295–311.
1179 https://doi.org/https://doi.org/10.1016/j.quascirev.2007.10.014

1180 Schildgen, T.F., Phillips, W.M., Purves, R.S., 2005. Simulation of snow shielding corrections for
1181 cosmogenic nuclide surface exposure studies. Geomorphology 64, 67–85.
1182 https://doi.org/10.1016/J.GEOMORPH.2004.05.003

1183 Schimmelpfennig, I., Benedetti, L., Garreta, V., Pik, R., Blard, P.-H., Burnard, P., Bourlès, D., Finkel, R.,
1184 Ammon, K., Dunai, T., 2011. Calibration of cosmogenic 36Cl production rates from Ca and K
1185 spallation in lava flows from Mt. Etna (38°N, Italy) and Payun Matru (36°S, Argentina). Geochim.
1186 Cosmochim. Acta 75, 2611–2632. https://doi.org/https://doi.org/10.1016/j.gca.2011.02.013

1187 Schlagenhauf, A., Gaudemer, Y., Benedetti, L., Manighetti, I., Palumbo, L., Schimmelpfennig, I., Finkel,
1188 R., Pou, K., 2010. Using in situ Chlorine-36 cosmonuclide to recover past earthquake histories
1189 on limestone normal fault scarps: a reappraisal of methodology and interpretations. Geophys. J.
1190 Int. 182, 36–72. https://doi.org/10.1111/j.1365-246X.2010.04622.x

1191 Schmidt, S., Hetzel, R., Kuhlmann, J., Mingorance, F., Ramos, V.A., 2011. A note of caution on the use
1192 of boulders for exposure dating of depositional surfaces. Earth Planet. Sci. Lett. 302, 60–70.
1193 https://doi.org/10.1016/j.epsl.2010.11.039

1194 Smart, P.L., 1991. Uranium series dating, in: Smart, P.L., Frances, P.D. (Eds.), A Users Guide. Technical
1195 Guide. No. 4. Quaternary Research Association, pp. 45–83.

1196 Stone, J.O., Allan, G.L., Fifield, L.K., Cresswell, R.G., 1996. Cosmogenic chlorine-36 from calcium
1197 spallation. Geochim. Cosmochim. Acta 60, 679–692. https://doi.org/10.1016/0016-
1198 7037(95)00429-7

1199 Styllas, M.N., Schimmelpfennig, I., Benedetti, L., Ghilardi, M., Aumaître, G., Bourlès, D., Keddadouche,
1200 K., 2018. Late-glacial and Holocene history of the northeast Mediterranean mountain glaciers -
1201 New insights from in situ-produced 36Cl-based cosmic ray exposure dating of paleo-glacier
1202 deposits on Mount Olympus, Greece. Quat. Sci. Rev. 193, 244–265.
1203 https://doi.org/https://doi.org/10.1016/j.quascirev.2018.06.020

1204 Šifrer, M., 1959. Obseg pleistocenske poledenitve na Notranjskem Snežniku. Geogr. Zb. 5, 27–83.

1205 Telbisz, T., Tóth, G., Ruban, D.A., Gutak, J.M., 2019. Notable Glaciokarsts of the World, in:
1206 Glaciokarsts. Springer Geography. Springer, Cham, pp. 373–499.

1207 Thomas, F., Godard, V., Bellier, O., Benedetti, L., Ollivier, V., Rizza, M., Guillou, V., Hollender, F.,
1208 Aumaître, G., Bourlès, D.L., Keddadouche, K., 2018. Limited influence of climatic gradients on
1209 the denudation of a Mediterranean carbonate landscape. Geomorphology 316, 44–58.
1210 https://doi.org/10.1016/J.GEOMORPH.2018.04.014

1211 Veress, M., 2009. Karst Environments. Karren Formation in High Mountains. Springer, Dordrecht.

1212 Vogel, H., Wagner, B., Zanchetta, G., Sulpizio, R., Rosén, P., 2010. A paleoclimate record with
1213 tephrochronological age control for the last glacial-interglacial cycle from Lake Ohrid, Albania
1214 and Macedonia. J. Paleolimnol. 44, 295–310. https://doi.org/10.1007/s10933-009-9404-x

1215 Vojnogeografski institut, 1969. Atlas klime Socijalističke Federativne Republike Jugoslavije.

1216 Wallinga, J., Cunningham, A., 2015. Luminescence Dating, Uncertainties and Age Range, in: Rink,
1217 W.J., Thompson, J.W. (Eds.), Encyclopedia of Scientific Dating Methods. Springer, pp. 440–445.
1218 https://doi.org/10.1007/978-94-007-6304-3_197

1219 WGMS, 2016. World Glacier Monitoring Service [WWW Document]. URL
1220 https://wgms.ch/products_ref_glaciers/south-cascade-glacier-pacific-coast-range/

1221 Woodward, J.C., Macklin, M.G., Smith, G.R., 2004. Pleistocene glaciation in the mountains of Greece,
1222 in: Developments in Quaternary Science|Dev. Quat. Sci. Elsevier Science, United Kingdom, pp.
1223 155–173. https://doi.org/10.1016/S1571-0866(04)80066-6

1224 Žebre, M., Stepišnik, U., 2015. Glaciokarst landforms and processes of the southern Dinaric Alps.
1225 Earth Surf. Process. Landforms 40, 1493–1505. https://doi.org/10.1002/esp.3731

1226 Žebre, M., Stepišnik, U., 2014. Reconstruction of Late Pleistocene glaciers on Mount Lovćen,
1227 Montenegro. Quat. Int. 353, 225–235. https://doi.org/10.1016/j.quaint.2014.05.006

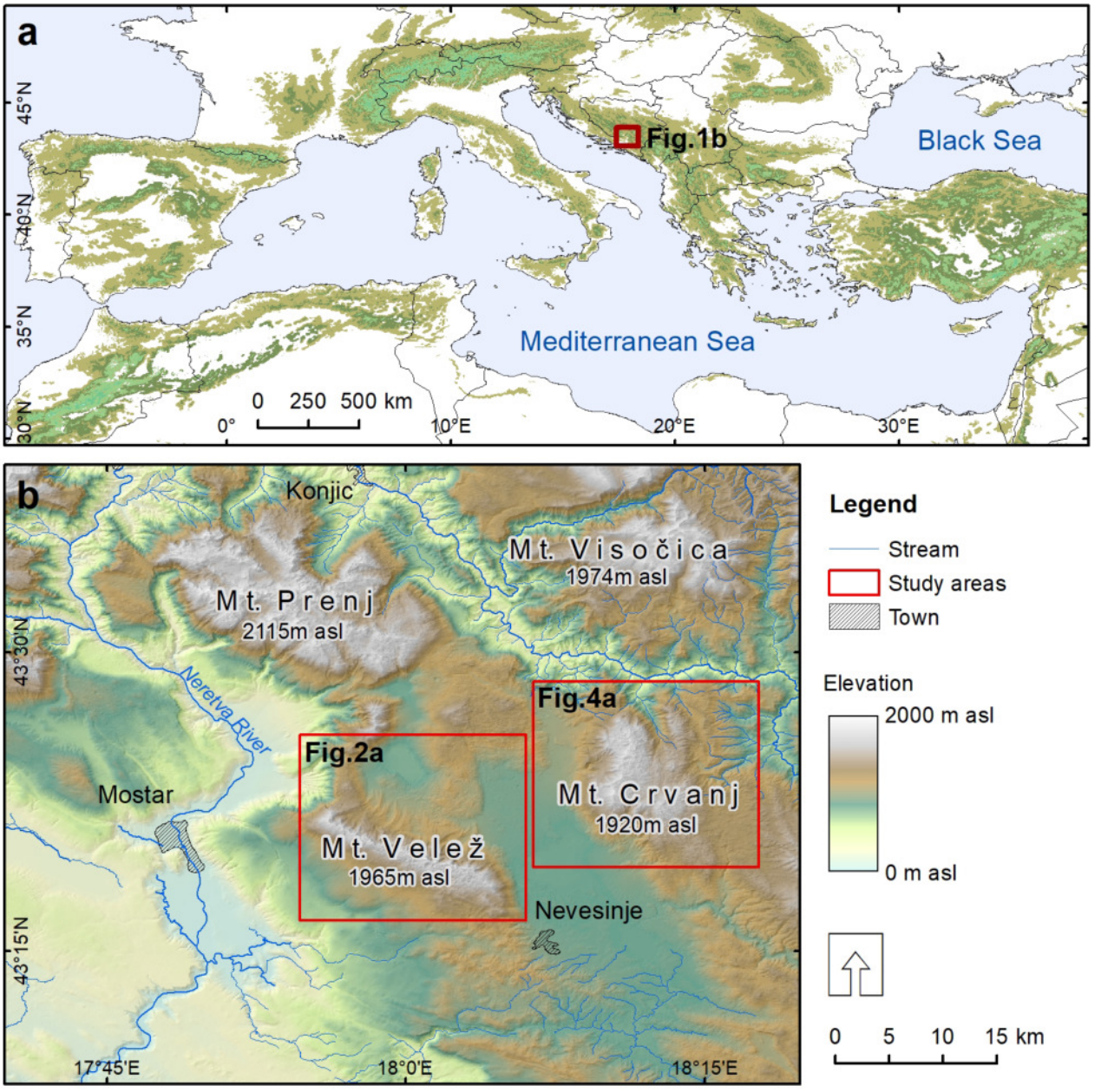
a
45°N
40°N
35°N
30°N
Fig.1b
Black Sea
Mediterranean Sea
0 250 500 km
0°
10°E
20°E
30°E
b
Konjic
Mt. Visočica
1974m asl
Mt. Prenj
2115m asl
43°30'N
Neretva River
Fig.4a
Fig.2a
Mostar
Mt. Crvanj
1920m asl
Mt. Velež
1965m asl
Nevesinje
43°15'N
17°45'E
18°0'E
18°15'E
Legend
Stream
Study areas
Town
Elevation
2000 m asl
0 m asl
0 5 10 15 km

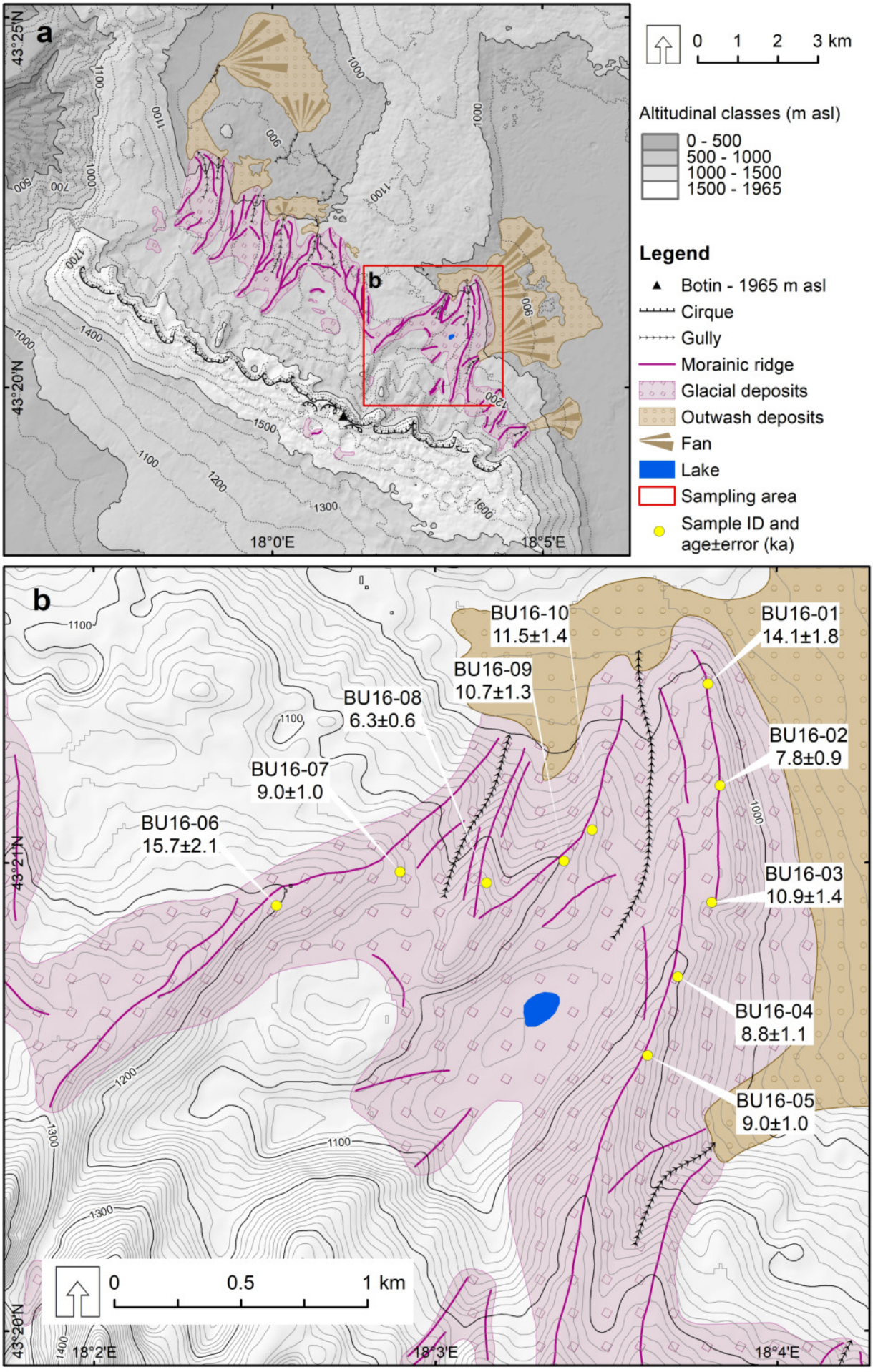
a
b
43°25'N
43°20'N
18°0'E
18°5'E
0 1 2 3 km
Altitudinal classes (m asl)
0 - 500
500 - 1000
1000 - 1500
1500 - 1965
Legend
Botin - 1965 m asl
Cirque
Gully
Morainic ridge
Glacial deposits
Outwash deposits
Fan
Lake
Sampling area
Sample ID and age±error (ka)
BU16-10 11.5±1.4
BU16-01 14.1±1.8
BU16-09 10.7±1.3
BU16-08 6.3±0.6
BU16-02 7.8±0.9
BU16-07 9.0±1.0
BU16-06 15.7±2.1
BU16-03 10.9±1.4
BU16-04 8.8±1.1
BU16-05 9.0±1.0
0 0.5 1 km
43°21'N
43°20'N
18°2'E
18°3'E
18°4'E

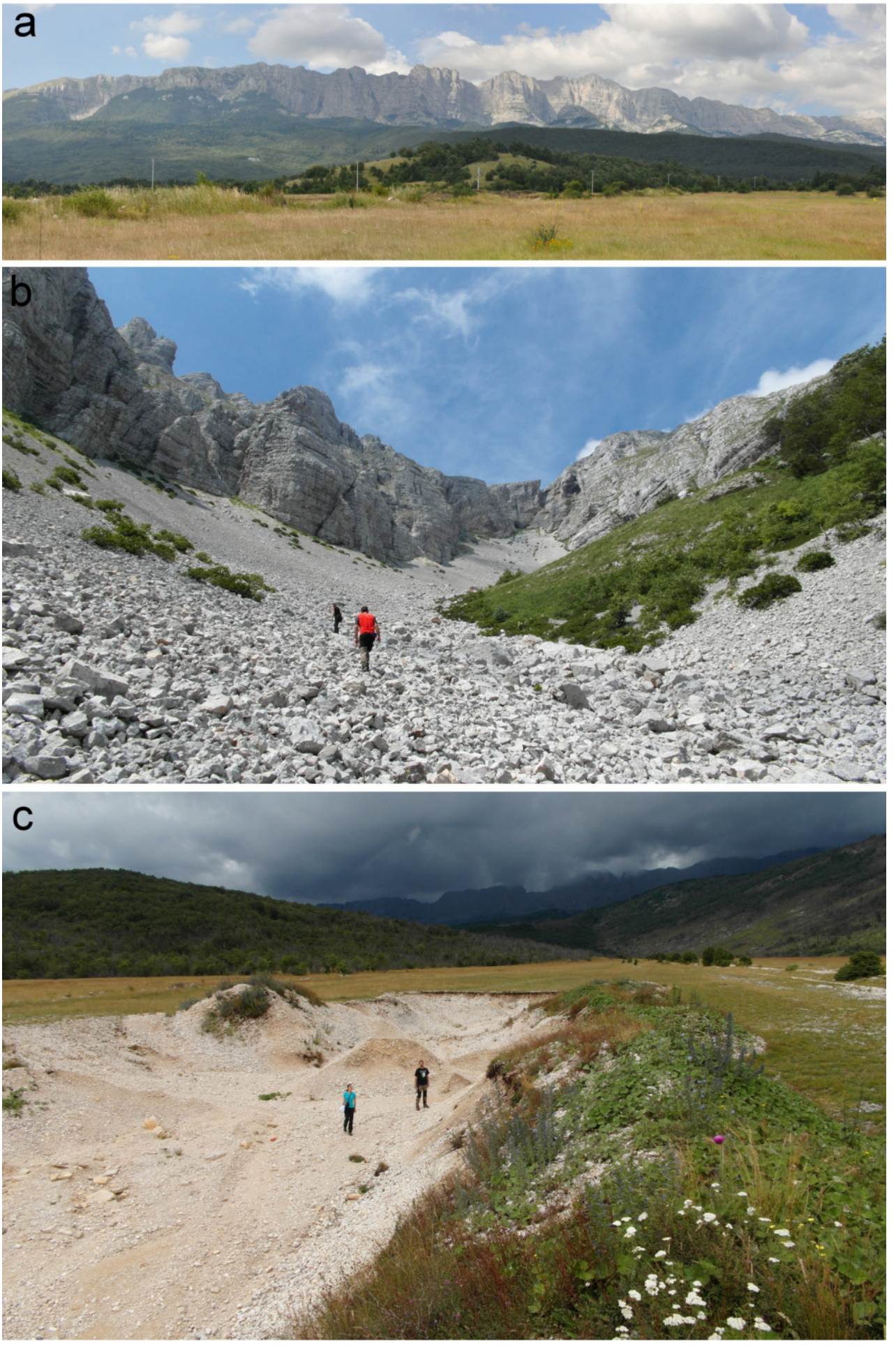
a
b
c

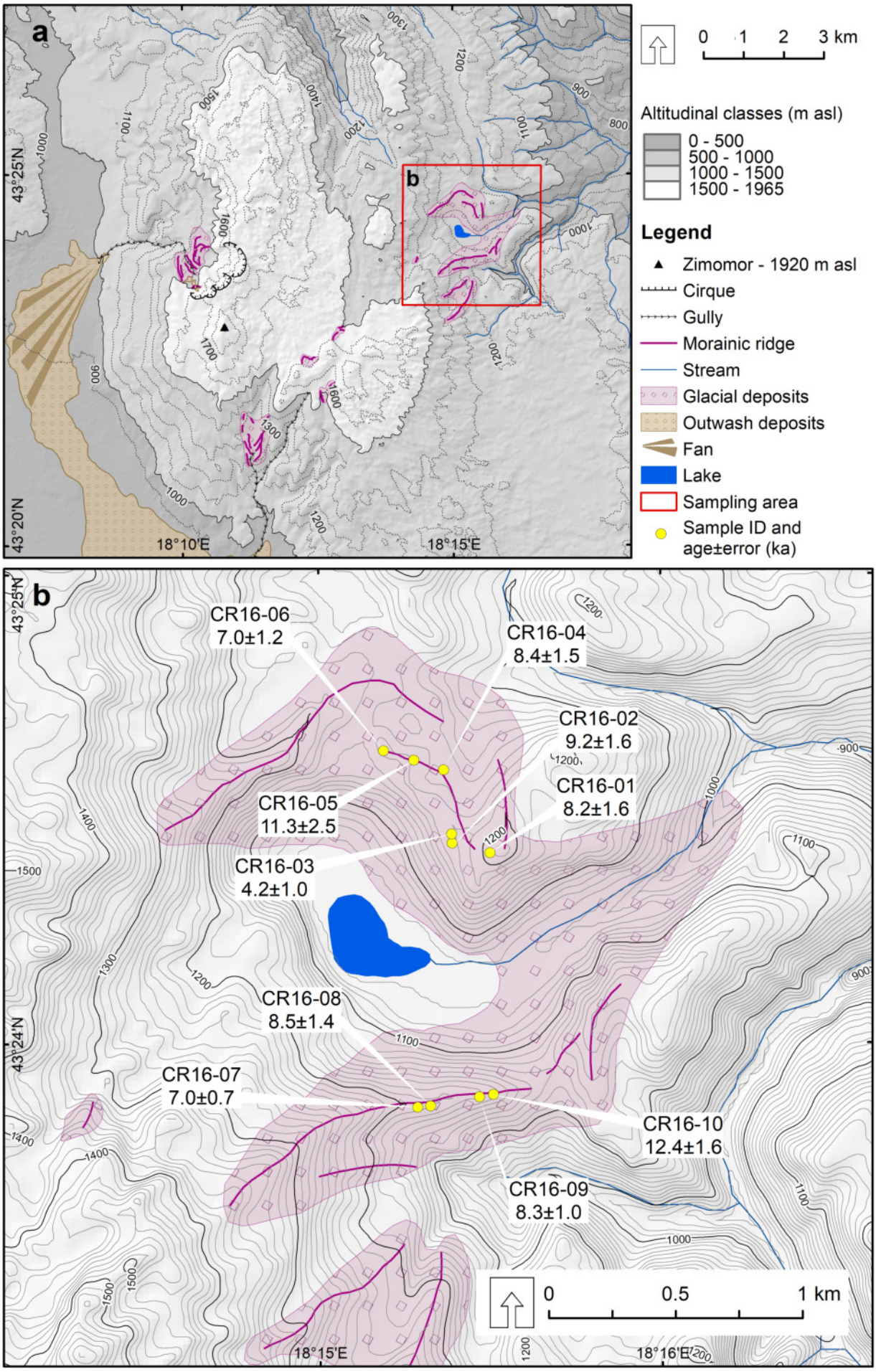
a
b
43°25'N
43°20'N
18°10'E
18°15'E
0 1 2 3 km
Altitudinal classes (m asl)
0 - 500
500 - 1000
1000 - 1500
1500 - 1965
Legend
Zimomor - 1920 m asl
Cirque
Gully
Morainic ridge
Stream
Glacial deposits
Outwash deposits
Fan
Lake
Sampling area
Sample ID and age±error (ka)
CR16-06 7.0±1.2
CR16-04 8.4±1.5
CR16-02 9.2±1.6
CR16-01 8.2±1.6
CR16-05 11.3±2.5
CR16-03 4.2±1.0
CR16-08 8.5±1.4
CR16-07 7.0±0.7
CR16-10 12.4±1.6
CR16-09 8.3±1.0
43°24'N
18°16'E
0 0.5 1 km


a


b


c


d


BU16-01 (14.1 ± 1.8 ka)


BU16-02 (7.8 ± 0.9 ka)


BU16-03 (10.9 ± 1.4 ka)


BU16-04 (8.8 ± 1.1 ka)


BU16-05 (9.0 ± 1.0 ka)


BU16-06 (15.7 ± 2.1 ka)


BU16-07 (9.0 ± 1.0 ka)


BU16-08 (6.3 ± 0.6 ka)


BU16-09 (10.7 ± 1.3 ka)


BU16-10 (11.5 ± 1.4 ka)

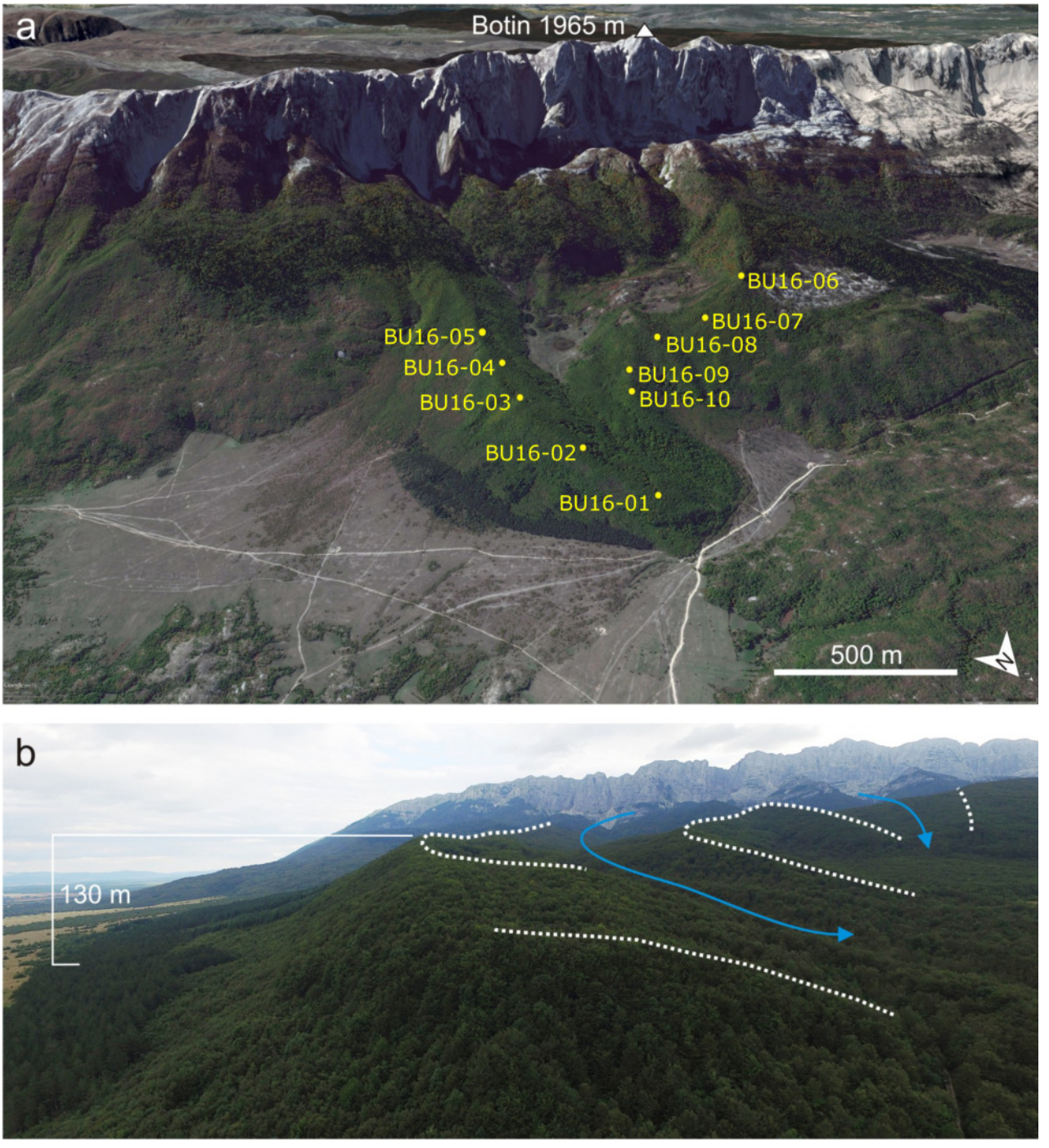
a
Botin 1965 m
BU16-06
BU16-07
BU16-08
BU16-09
BU16-10
BU16-05
BU16-04
BU16-03
BU16-02
BU16-01
500 m
N
b
130 m

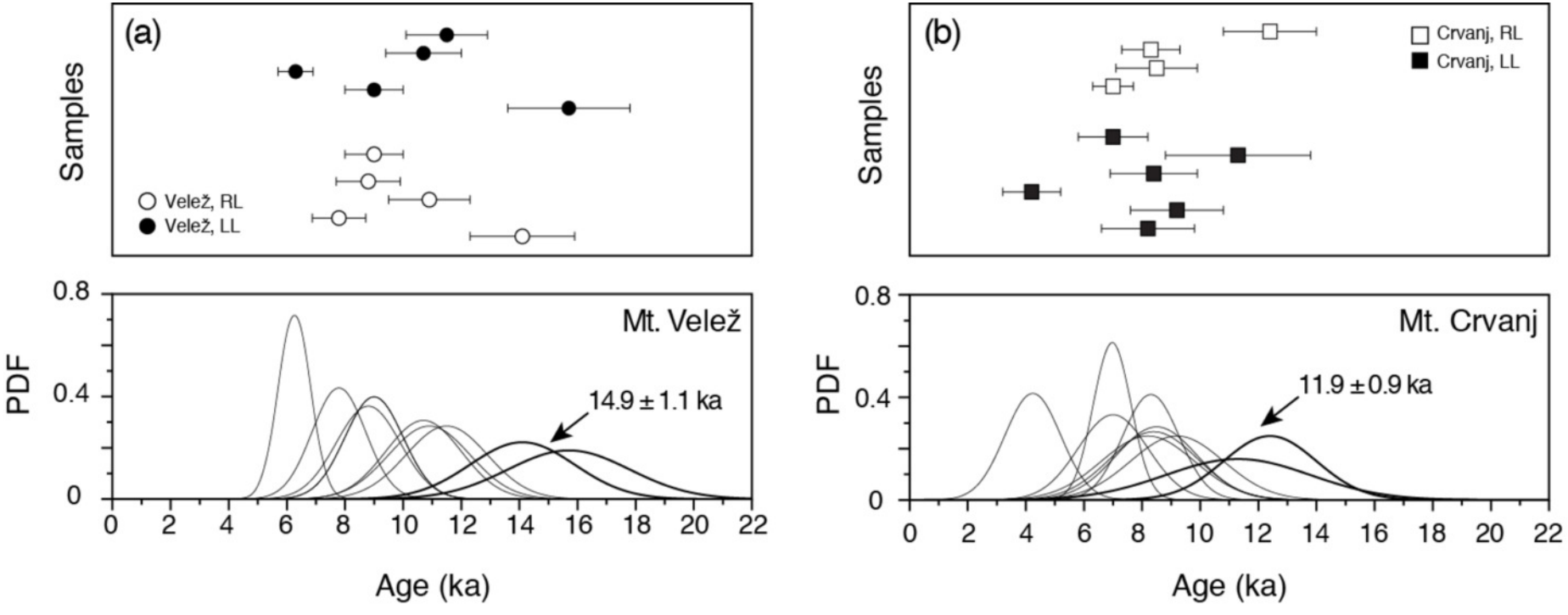
(a)
Samples
Velež, RL
Velež, LL
(b)
Crvanj, RL
Crvanj, LL
Samples
PDF
0.8
0.4
0
Mt. Velež
14.9 ± 1.1 ka
Mt. Crvanj
11.9 ± 0.9 ka
0 2 4 6 8 10 12 14 16 18 20 22
Age (ka)


CR16-01 (8.2 ± 1.6 ka)


CR16-02 (9.2 ± 1.6 ka)


CR16-03 (4.2 ± 1.0 ka)


CR16-04 (8.4 ± 1.5 ka)


CR16-05 (11.3 ± 2.5 ka)


CR16-06 (7.0 ± 1.2 ka)


CR16-07 (7.0 ± 0.7 ka)


CR16-08 (8.5 ± 1.4 ka)


CR16-10 (12.4 ± 1.6 ka)


CR16-09 (8.3 ± 1.0 ka)

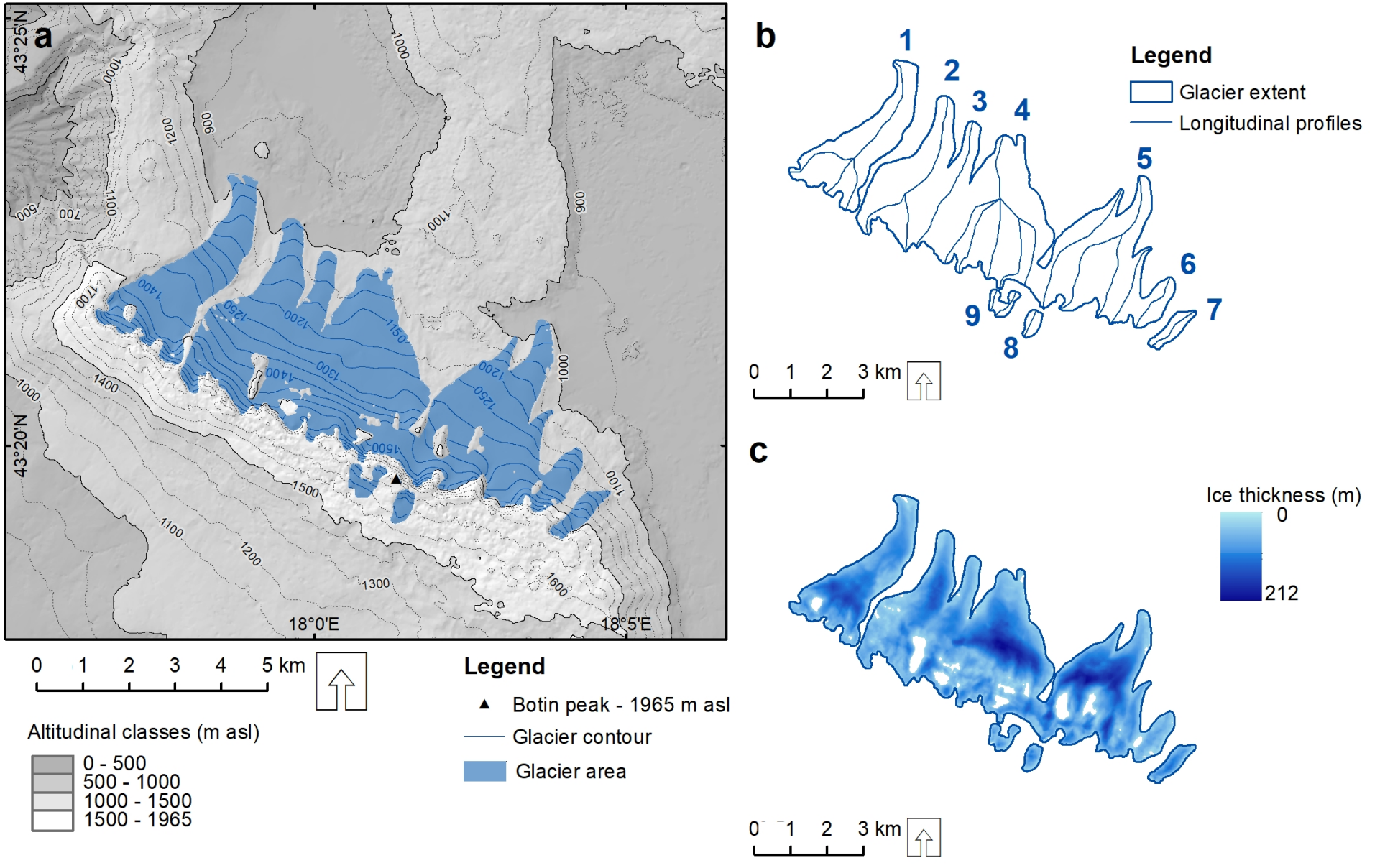
a
43°25'N
43°20'N
18°0'E
18°5'E
0 1 2 3 4 5 km
Altitudinal classes (m asl)
0 - 500
500 - 1000
1000 - 1500
1500 - 1965
Legend
Botin peak - 1965 m asl
Glacier contour
Glacier area
b
1
2
3
4
5
6
7
8
9
Legend
Glacier extent
Longitudinal profiles
0 1 2 3 km
c
Ice thickness (m)
0
212
0 1 2 3 km

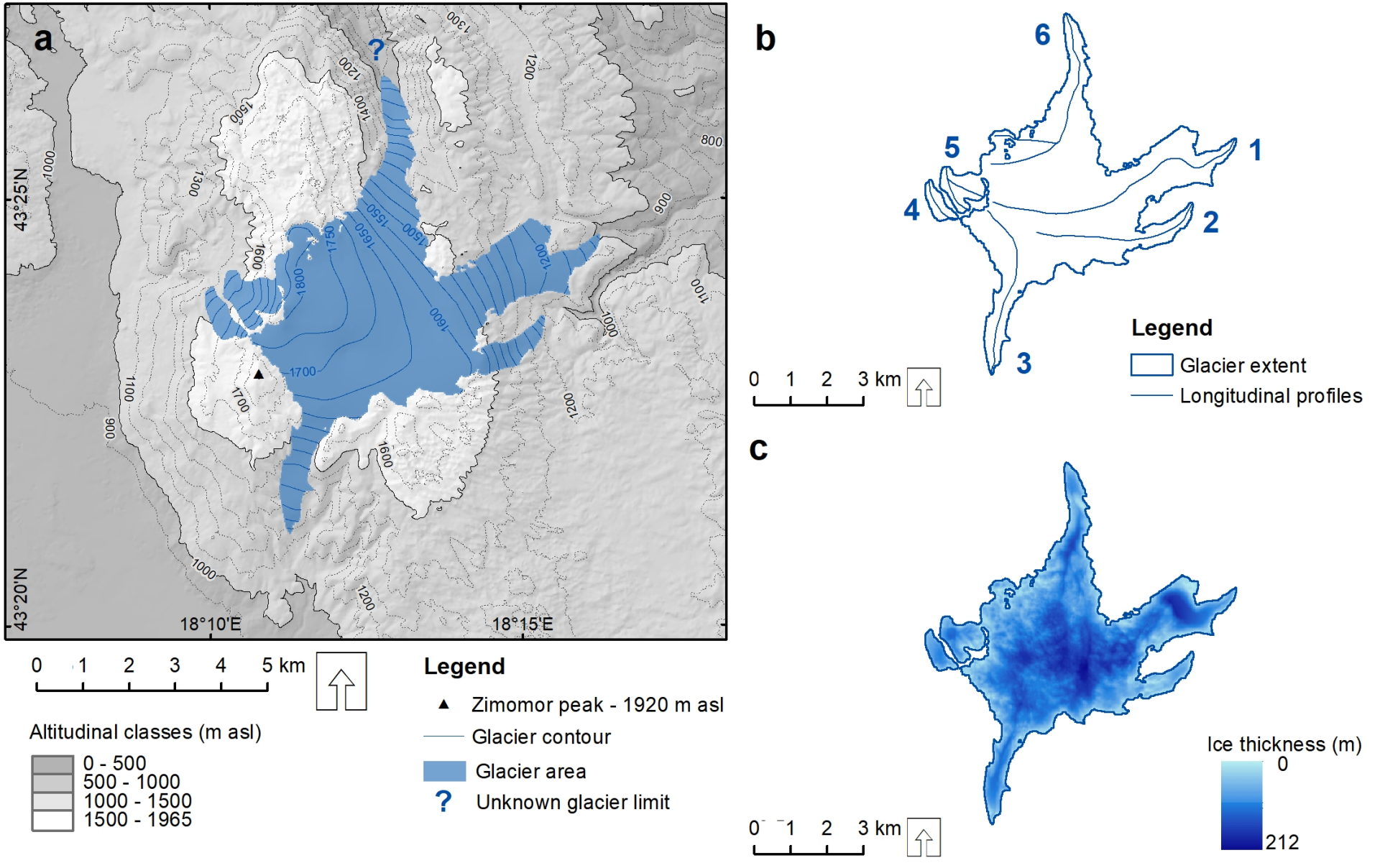
a
b
c
43°25'N
43°20'N
18°10'E
18°15'E
0 1 2 3 4 5 km
Altitudinal classes (m asl)
0 - 500
500 - 1000
1000 - 1500
1500 - 1965
Legend
Zimomor peak - 1920 m asl
Glacier contour
Glacier area
Unknown glacier limit
1
2
3
4
5
6
0 1 2 3 km
Legend
Glacier extent
Longitudinal profiles
0 1 2 3 km
Ice thickness (m)
0
212

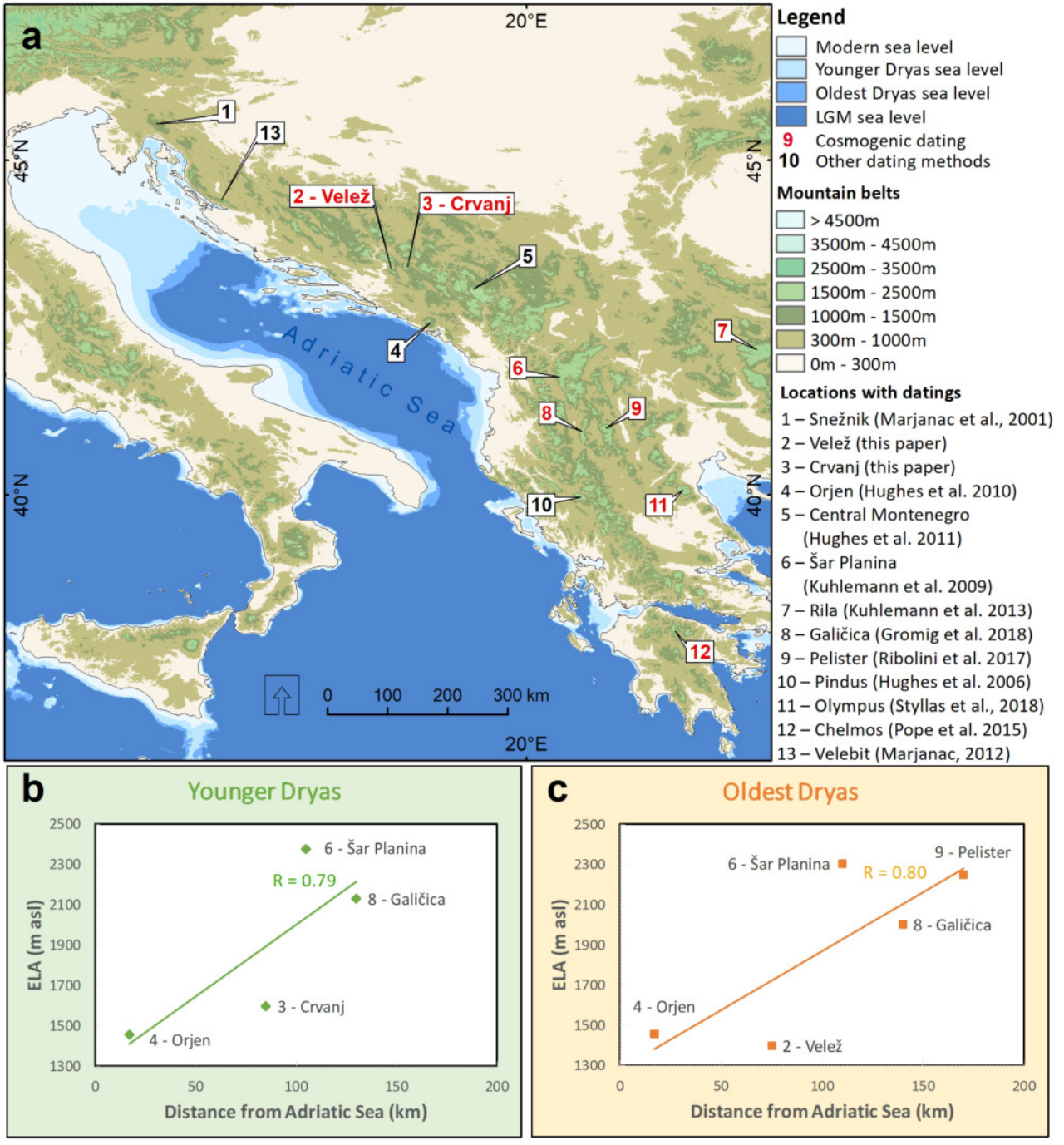
a
20°E
45°N
40°N
Adriatic Sea
0 100 200 300 km
1
13
2 - Velež
3 - Crvanj
5
4
6
7
8
9
10
11
12
Legend
Modern sea level
Younger Dryas sea level
Oldest Dryas sea level
LGM sea level
9 Cosmogenic dating
10 Other dating methods
Mountain belts
> 4500m
3500m - 4500m
2500m - 3500m
1500m - 2500m
1000m - 1500m
300m - 1000m
0m - 300m
Locations with datings
1 – Snežnik (Marjanac et al., 2001)
2 – Velež (this paper)
3 – Crvanj (this paper)
4 – Orjen (Hughes et al. 2010)
5 – Central Montenegro (Hughes et al. 2011)
6 – Šar Planina (Kuhlemann et al. 2009)
7 – Rila (Kuhlemann et al. 2013)
8 – Galičica (Gromig et al. 2018)
9 – Pelister (Ribolini et al. 2017)
10 – Pindus (Hughes et al. 2006)
11 – Olympus (Styllas et al., 2018)
12 – Chelmos (Pope et al. 2015)
13 – Velebit (Marjanac, 2012)
b
Younger Dryas
ELA (m asl)
Distance from Adriatic Sea (km)
R = 0.79
6 - Šar Planina
8 - Galičica
3 - Crvanj
4 - Orjen
c
Oldest Dryas
ELA (m asl)
Distance from Adriatic Sea (km)
R = 0.80
9 - Pelister
6 - Šar Planina
8 - Galičica
4 - Orjen
2 - Velež

	Sample ID	Latitude (WGS84)	Longitude (WGS84)	Elevation	Boulder dimensions (LxWxH)	Sample thickness	Topography correction factor
		°N (DD)	°E (DD)	(m, asl)	(m)	(cm)	
1	BU16-01	43.3565	18.0583	1010	2x2.5x1.6	3	0.9986
2	BU16-02	43.3529	18.0589	1055	1x1x0.5	3	0.9970
3	BU16-03	43.3487	18.0585	1070	1.5x0.8x0.6	3	0.9990
4	BU16-04	43.3461	18.0568	1105	1.5x1.5x0.6	2.5	0.9982
5	BU16-05	43.3433	18.0553	1130	2x1.8x1.2	3	0.9971
6	BU16-06	43.3486	18.0372	1200	2.4x3x1.5	2	0.9983
7	BU16-07	43.3498	18.0433	1145	1.5x1x0.6	2	0.9897
8	BU16-08	43.3494	18.0475	1130	1.5x0.8x0.4	2	0.9886
9	BU16-09	43.3502	18.0513	1095	1x0.8x0.5	4	0.9915
10	BU16-10	43.3513	18.0526	1075	1x0.5x0.45	2	0.9939
11	CR16-01	43.4069	18.2533	1208	1x2.5x1	3	0.9956
12	CR16-02	43.4072	18.2515	1180	0.9x0.4x0.6	3	0.9927
13	CR16-03	43.4076	18.2514	1180	1x1.5x0.2	3	0.9946
14	CR16-04	43.4098	18.2510	1170	1.7x1.2x0.6	3	0.9935
15	CR16-05	43.4102	18.2496	1170	3x4x1.5	3	0.9947
16	CR16-06	43.4105	18.2481	1175	1.5x1.8x0.5	3	0.9925
17	CR16-07	43.3979	18.2497	1187	1x1.5x1	4	0.9824
18	CR16-08	43.3979	18.2504	1202	1x1x0.4	4	0.9866
19	CR16-09	43.3982	18.2527	1187	2.5x2x1.5	4	0.9960
20	CR16-10	43.3983	18.2534	1187	1.4x1x1	3	0.9960

		Major elements											Trace elements				
	Sample ID	Al_2O_3	CaO	Fe_2O_3	K_2O	MgO	MnO	Na_2O	P_2O_5	SiO_2	TiO_2	CO_2 (LOI)	Sm	Gd	U	Th	Cl
		(wt. %)	(wt. %)	(wt. %)	(wt. %)	(wt. %)	(wt. %)	(wt. %)	(wt. %)	(wt. %)	(wt. %)	(wt. %)	(ppm)	(ppm)	(ppm)	(ppm)	(ppm)
1	BU16-01	0.02	54.87	0.04	0.01	0.79	0.01	0.02	0.01	0.38	0.01	43.80	0.05	0.05	2.30	0.20	20.8 ± 1.9
2	BU16-02	0.11	54.72	0.11	0.03	0.89	0.01	0.03	0.01	0.42	0.01	43.60	0.05	0.05	1.70	0.20	37.5 ± 3.4
3	BU16-03	0.29	54.17	0.12	0.09	0.69	0.01	0.01	0.01	0.96	0.01	43.60	0.13	0.19	2.60	0.20	25.6 ± 2.3
4	BU16-04	0.02	55.21	0.04	0.01	0.55	0.01	0.01	0.01	0.43	0.01	43.70	0.05	0.05	1.60	0.20	12.9 ± 1.2
5	BU16-05	0.01	54.28	0.04	0.01	1.55	0.01	0.01	0.01	0.19	0.01	43.90	0.05	0.05	0.70	0.20	22.9 ± 2.1
6	BU16-06	0.01	55.65	0.04	0.01	0.47	0.01	0.01	0.01	0.18	0.01	43.60	0.05	0.05	1.50	0.20	18.6 ± 1.7
7	BU16-07	0.04	53.66	0.04	0.01	2.14	0.01	0.02	0.01	0.33	0.01	43.70	0.05	0.05	2.10	0.20	27.2 ± 2.5
8	BU16-08	0.01	55.06	0.04	0.01	0.50	0.01	0.03	0.01	0.24	0.01	44.10	0.05	0.05	1.50	0.20	21.7 ± 2.0
9	BU16-09	0.03	54.59	0.04	0.01	0.74	0.01	0.02	0.01	0.44	0.01	44.10	0.05	0.05	1.10	0.20	19.5 ± 1.8
10	BU16-10	0.02	54.82	0.04	0.01	0.68	0.01	0.02	0.01	0.25	0.01	44.10	0.05	0.06	2.10	0.20	20.5 ± 1.9
11	CR16-01	0.37	34.16	0.15	0.13	17.48	0.01	0.04	0.06	1.11	0.02	46.10	1.20	1.46	3.10	0.40	410.7 ± 37.1
12	CR16-02	0.98	26.51	0.34	0.36	15.25	0.01	0.04	0.07	17.28	0.05	38.80	1.03	1.04	1.40	1.00	139.3 ± 12.6
13	CR16-03	0.16	32.27	0.19	0.06	19.21	0.01	0.03	0.02	0.65	0.01	47.10	0.33	0.59	1.20	0.20	450.0 ± 40.3
14	CR16-04	0.29	32.69	0.14	0.12	18.68	0.01	0.05	0.06	1.00	0.02	46.60	0.79	1.00	4.80	0.30	283.5 ± 25.4
15	CR16-05	0.58	30.49	0.29	0.20	17.45	0.01	0.04	0.02	6.57	0.03	44.00	0.54	0.55	0.80	0.50	279.5 ± 25.1
16	CR16-06	0.44	32.24	0.19	0.16	18.38	0.01	0.04	0.05	2.21	0.03	45.90	0.49	0.59	3.60	0.40	340.3 ± 30.6
17	CR16-07	0.15	54.28	0.08	0.06	0.76	0.01	0.02	0.03	0.65	0.01	43.90	0.41	0.52	0.80	0.20	61.4 ± 5.6
18	CR16-08	0.11	43.59	0.14	0.04	9.79	0.01	0.02	0.06	0.52	0.01	45.50	0.29	0.30	0.50	0.20	155.7 ± 14.1
19	CR16-09	0.08	54.02	0.07	0.03	1.10	0.01	0.02	0.05	0.42	0.01	44.20	0.58	0.76	0.80	0.20	31.8 ± 2.9
20	CR16-10	0.04	54.39	0.04	0.02	0.93	0.01	0.02	0.03	0.38	0.01	44.10	0.26	0.32	0.50	0.20	63.8 ± 5.8

Sample ID	Landform	^{36}Cl (measured)	Contemporary depth average total production rate	SURFACE EXPOSURE AGES				Landform age calculated using erosion correction of 40 mm ka-1
				erosion not corrected (0 mm ka^{-1})	erosion corrected (20 mm ka^{-1})	erosion corrected (40 mm ka^{-1})	erosion corrected (60 mm ka^{-1})	
		(10^4 atoms g^{-1} rock)	(atoms g^{-1} rock a^{-1})	(ka)	(ka)	(ka)	(ka)	(ka)
Mt. Velež								
BU16-01	Budijevača, right lateral moraine	46.53 ± 1.54	41.8	9.9 ± 0.9	11.3 ± 1.1	**14.1 ± 1.8**	21.0 ± 5.0	
BU16-02	Budijevača, right lateral moraine	34.46 ± 1.77	44.8	6.8 ± 0.6	7.1 ± 0.7	7.8 ± 0.9	9.0 ± 1.3	
BU16-03	Budijevača, right lateral moraine	41.84 ± 1.39	44.0	8.4 ± 0.7	9.2 ± 0.9	10.9 ± 1.4	14.1 ± 2.3	**14.1±1.8**
BU16-04	Budijevača, right lateral moraine	35.17 ± 1.37	44.7	7.0 ± 0.6	7.7 ± 0.7	8.8 ± 1.1	10.9 ± 1.6	
BU16-05	Budijevača, right lateral moraine	37.57 ± 1.17	45.7	7.3 ± 0.6	7.9 ± 0.7	9.0 ± 1.0	11.0 ± 1.8	
BU16-06	Budijevača, left lateral moraine	58.24 ± 1.71	49.3	10.5 ± 0.9	12.2 ± 1.2	**15.7 ± 2.1**	27.5 ± 8.6	
BU16-07	Budijevača, left lateral moraine	39.59 ± 1.32	46.0	7.6 ± 0.6	8.1 ± 0.7	9.0 ± 1.0	11.4 ± 1.8	
BU16-08	Budijevača, left lateral moraine	28.09 ± 1.22	46.0	5.5 ± 0.5	5.8 ± 0.5	6.3 ± 0.6	7.0 ± 0.8	**15.7±2.1**
BU16-09	Budijevača, left lateral moraine	40.27 ± 1.36	43.9	8.1 ± 0.7	9.0 ± 0.9	10.7 ± 1.3	13.9 ± 2.2	
BU16-10	Budijevača, left lateral moraine	42.79 ± 1.68	44.0	8.6 ± 0.8	9.6 ± 1.0	11.5 ± 1.4	15.3 ± 2.7	
Mt. Crvanj								
CR16-01	Crvanj, lateral above the lake	116.95 ± 3.61	75.8	12.0 ± 1.8	8.5 ± 1.4	8.2 ± 1.6	8.6 ± 2.1	
CR16-02	Crvanj, lateral above the lake	52.69 ± 1.67	38.9	11.5 ± 1.4	9.2 ± 1.4	9.2 ± 1.6	10.2 ± 2.3	
CR16-03	Crvanj, lateral above the lake	61.30 ± 9.51	78.7	6.1 ± 1.3	5.0 ± 1.0	4.2 ± 1.0	4.7 ± 1.0	**11.3±2.5**
CR16-04	Crvanj, lateral above the lake	97.27 ± 3.24	59.4	12.0 ± 1.7	8.7 ± 1.5	8.4 ± 1.5	8.9 ± 2.2	
CR16-05	Crvanj, lateral above the lake	105.07 ± 3.69	57.8	15.6 ± 2.3	11.2 ± 1.8	**11.3 ± 2.5**	13.0 ± 4.1	
CR16-06	Crvanj, lateral above the lake	92.05 ± 2.82	66.0	10.2 ± 1.6	7.4 ± 1.1	7.0 ± 1.2	7.1 ± 1.5	
CR16-07	Crvanj, right lateral moraine	37.34 ± 1.37	51.4	6.4 ± 0.5	6.6 ± 0.6	7.0 ± 0.7	8.0 ± 1.0	
CR16-08	Crvanj, right lateral moraine	59.78 ± 1.82	55.2	9.5 ± 1.1	8.3 ± 1.1	8.5 ± 1.4	9.4 ± 1.9	**12.4±1.6**
CR16-09	Crvanj, right lateral moraine	38.21 ± 1.31	48.4	7.0 ± 0.6	7.5 ± 0.6	8.3 ± 1.0	9.9 ± 1.5	
CR16-10	Crvanj, right lateral moraine	60.16 ± 1.87	52.4	10.2 ± 0.8	11.0 ± 1.0	**12.4 ± 1.6**	16.5 ± 3.4	

Velež

	AABR 1.9±0.81
Glacier 1	1287 (+ 40 / -20)
Glacier 2	1271 (+ 40 / -20)
Glacier 3	1216 (+ 30 / -10)
Glacier 4	1284 (+ 30 / -20)
Glacier 5	1265 (+ 30 / -20)
Glacier 6	1327 (+ 20 / -20)
Glacier 7	1393 (+ 30 / -10)
Glacier 8	1724 (+ 10 / -10)
Glacier 9	1728 (+ 10 / -10)
Mean	**1388** (σ 186)

Crvanj

	AABR 1.9±0.81
Glacier 1	1468 (+ 60 / -30)
Glacier 2	1577 (+ 30 / -20)
Glacier 3	1541 (+ 40 / -20)
Glacier 4	1553 (+ 20 / 0)
Glacier 5	1607 (+ 20 / -10)
Glacier 6	1500 (+ 50 / -30)
Mean	**1541** (σ 46)

Velež

Temperature depression (ºC)	*Mean annual temperature at ELA (ºC)*	Annual melt (mm w.e.)	
		Annual Range = 18.9 ºC	*150% Annual Range = 28.35 ºC*
0	5.4	9304	11295
4	1.4	5601	7837
5	0.4	4807	7058
6	-0.6	4064	6313
7	-1.6	3371	5601
8	-2.6	2729	4923
9	**-3.6**	**2140**	4280
10	**-4.6**	**1605**	3671
11	-5.6	1128	3098
12	-6.6	714	2561
13	-7.6	372	2063
14	-8.6	115	1604
15	-9.6	0	1188

Crvanj

Temperature depression (ºC)	*Mean annual temperature at ELA (ºC)*	Annual melt (mm w.e.)	
		Annual Range = 18.9 ºC	*150% Annual Range = 28.35 ºC*
0	4.4	8295	10378
4	0.4	4807	7058
5	-0.6	4064	6313
6	-1.6	3371	5601
7	-2.6	2729	4923
8	**-3.6**	**2140**	4280
9	**-4.6**	**1605**	3671
10	-5.6	1128	3098
11	-6.6	714	2561
12	-7.6	372	2063
13	-8.6	115	1604
14	-9.6	0	1188
15	-10.6	0	817

Mountain	Dating method	Age	Erosion rate	Number of samples	Reference
Snežnik (Croatia)	14C	LGM (*18.7 ±1.0 cal kyr BP)	/	1 (animal bone in outwash fan)	Marjanac et al., 2001
Pindus (Greece)	U-series	MIS 12 (>350 to 71 ka), MIS 6 (131.3 to 80.5 ka)	/	28 from at least 11 landforms (calcite cement from moraines and alluvial deposits)	Hughes et al., 2006; Woodward et al., 2004
Šar Planina (FYROM)	10Be cosmogenic exposure dating	LGM (19.4 ± 3.2 to 12.4 ± 1.7 ka), Oldest Dryas (14.7 ± 2.1 ka) Younger Dryas (12.7 ± 1.9 ka)	10 mm/ka	8 from at least 6 landforms (moraine and rock glacier boulders)	Kuhlemann et al., 2009
Orjen (Montenegro)	U-series	MIS 12 (>350 to 324.0 ka), MIS 6 (124.6 to 102.4 ka), MIS 5d-2 (17.3 to 12.5 ka), Younger Dryas (9.6 to 8.0 ka)	/	12 from 7 landforms (calcite cement from moraines)	Hughes et al., 2010
Central Montenegro	U-series	MIS 12 (>350 ka; 396.6 to 38.8 ka), MIS 8 or 10 (231.9 to 58.8 ka), MIS 6 (120.2 to 88.1 ka) MIS 2 (13.4 ka), Younger Dryas (10.9 to 2.2 ka)	/	19 from 11 landforms (calcite cement from moraines)	Hughes et al., 2011
Velebit (Croatia)	U-series	MIS 12-6 (>350 to 61.5 ka)	/	9 from at least 6 landforms (calcite cement from moraines, paleocaverns, former ice wedges)	Marjanac, 2012; Marjanac&Marjanac, 2016
Rila (Bulgaria)	10Be cosmogenic exposure dating	LGM (23.5 to 14.4 ka)	0 mm/ka	10 from at least 6 landforms (moraine boulders)	Kuhlemann et al., 2013
Chelmos (Greece)	**36Cl cosmogenic exposure dating**	MIS 3 (39.9 ± 3.0 to 30.4 ± 2.2 ka), LGM (22.9 ±1.6 to 21.2 ± 1.6 ka), Younger Dryas (*CH10=12.6 ± 0.9, *CH11=10.2 ± 0.7 ka)	0 mm/ka	7 from 4 different landforms (moraine boulders)	Pope et al., 2015
Galičica (FYROM)	**36Cl cosmogenic exposure dating**	Younger Dryas (12.8 ± 1.4 to 11.3 ± 1.3 ka)	5 mm/ka	5 from 1 landform (moraine boulders)	Gromig et al., 2018
Pelister (FYROM)	10Be cosmogenic exposure dating	Oldest Dryas (15.56 ± 0.85 to 15.03 ± 0.85 ka)	0 mm/ka	3 from 1 landform (moraine boulders)	Ribolini et al., 2017
Olympus (Greece)	**36Cl cosmogenic exposure dating**	Lateglacial (3 phases: 15.5 ± 2.0 ka (*TZ03=16.35 ± 1.15 ka, *MK12=16.22 ± 1.13 ka), 13.5 ± 2.0 ka, 12.5 ± 1.5 ka), Holocene (3 phases: 9.6 ± 1.1 ka, 2.5 ± 0.3 ka, 0.64 ± 0.08ka)	5 mm/ka	20 from 11 landforms (moraine boulders, bedrock)	Styllas et al., 2018